Bulletin of Earthquake Engineering (2023) 21:397–432
https://doi.org/10.1007/s10518-022-01535-4

ORIGINAL ARTICLE

Fragility curves of Italian school buildings: derivation from L'Aquila 2009 earthquake damage via observational and heuristic approaches

Marco Di Ludovico[1] · Serena Cattari[2] · Gerardo Verderame[1] · Ciro Del Vecchio[3] · Daria Ottonelli[2] · Carlo Del Gaudio[1] · Andrea Prota[1] · Sergio Lagomarsino[2]

Received: 29 March 2022 / Accepted: 8 October 2022 / Published online: 1 November 2022

Abstract
Recent seismic events worldwide have demonstrated the high vulnerability of existing school buildings and the urgent need to have reliable tools for the rapid seismic performance assessment and damage and loss quantification. Indeed, the significant damage observed on structural and non-structural components may have a significant impact in terms of direct and indirect losses making critical the recovery of stricken communities. Although a significant amount of work has been done in developing fragility curves for the residential building stock, only few contributions clearly refer to school buildings that significantly differ in terms of the main characteristics from the residential ones. This research work proposes fragility curves for reinforced concrete and unreinforced masonry public school buildings typical of the Italian building stock, based on the damage observed in the aftermath of the 2009 L'Aquila earthquake. A comprehensive and unique database including data on damaged and undamaged school buildings (2037 records) in the Abruzzo region was built using data from four different sources. Due to limited amount of data, the fragility curves can be very sensitive to the method adopted for their derivation, thus three different approaches (i.e. empirical, empirical-binomial, heuristic) are considered in the paper and the results are compared. Finally, a direct comparison with fragility curves available in the literature for the Italian residential building stock is presented.

Keywords School buildings · Fragility curves · Vulnerability · Seismic risk · Masonry · Reinforced Concrete

1 Introduction

School buildings are essential for the life of communities because education is a key to developing character, and building social and life skills. They are not only the places for education of younger generations but also used for social activities and recovering after natural disasters. Thus, they are expected to be a safe place for children and for the entire

✉ Serena Cattari
serena.cattari@unige.it

Extended author information available on the last page of the article

communities. However, recent seismic events occurred worldwide clearly demonstrated that significant damage has been frequently detected in such buildings and that many threatened communities do not yet have earthquake-proof schools (Augenti et al. 2004; Goretti and Di Pasquale 2004; OECD 2004; Grant et al. 2007; Wang et al. 2007; Taylor et al. 2010; Nakano 2020). In particular, in the aftermath of recent Italian earthquakes (Di Ludovico et al. 2019a,b), the damage detected in public and strategic buildings pointed out the high levels of vulnerability and inadequate performance of these building. In several cases, the amount and level of damage resulted comparable to those of ordinary buildings and, consequently, the number of unusable buildings inadequate to allow a rapid recovery of daily activities. Similar unsatisfactory circumstances were recently detected in several other countries [e.g. Nepal (Gautam et al. 2020), and Iran (Azizi-Bondarabadi et al. 2016)].

In light of this, a significant effort has been devoted worldwide to develop projects for seismic rehabilitation of school buildings and promote the mitigation of vulnerability of both structural and non-structural components (e.g., WISS 2013; UNISDR 2014). Moreover, the need for derivation and a periodic update of the national risk assessment of school buildings is coherent with EU decision 1313 (2013) and responds to the specific requirement of the Sendai Framework for Disaster Risk Reduction 2015–2030.

The growing attention to this topic is also testified by various recent studies addressed to reduce risk and enhance resilience of school buildings (e.g., Gonzalez et al. 2020; D'Ayala et al. 2020). In particular, a significant effort has been recently devoted to studies aiming at the evaluation of fragility curves; indeed, they represent a sound tool to support large-scale analyses and scenarios and define suitable mitigation policies. In this context, the knowledge of typological and constructive characteristics of the building stock is crucial for reliable risk analyses, if fragility curves are used as a prediction tool.

Works available in literature are often based on mechanical approaches, either numerical or analytical (Michel et al. 2017; Hannewald et al. 2020; D'Ayala et al. 2020; Yekrangnia et al. 2021; Giordano et al. 2021a, b); even if no empirical evidence is provided by such approaches, they are considered suitable to capture the effects of specific features affecting the seismic vulnerability of buildings. Fragility curves based on the direct observation of damage have been recently developed in several studies addressed to building stock of different countries; however, they commonly refer to private ordinary buildings (Dolce et al. 2021; Martins and Silva 2021), while empirical fragility curves for public buildings are still lacking. This because the public building stock is scarce and scattered on the territory leading to critical issues in the derivation of reliable curves. Empirical fragility curves derived for school buildings can be found in Munoz et al. (2007) and Giordano et al. (2021a, b) for Peruvian and Nepalese schools, respectively. Although characterized by a limited amount of data, they certainly represent a valuable resource being based on direct observation of damage.

In Italy, a significant effort has been recently devoted by the Civil Protection Department and his competence centre ReLUIS (University Laboratories of Seismic Engineering) to the risk assessment not only of residential buildings but also of other strategic classes, such as schools and churches (Masi et al. 2021). In particular, within the work package WP4 "Seismic Risk Maps—MARS" of the 2019–2021 project, a task has been specifically targeted to the derivation of seismic fragility models for school buildings (Cattari et al. 2022). In this context, the present paper aims at the derivation of fragility curves from real observed data recorded after the 2009 L'Aquila earthquake. To this scope, the first section of the paper focuses on the issues related to the sample completeness; it describes the different sources of data used to create the database, which represents the indispensable basis for the derivation of reliable fragility curves (Sect. 2). Section 3 shows the procedure used

to determine the Damage Probability Matrix (DPM) from the damage data collected with AeDES form (Baggio et al. 2007), namely the adopted damage conversion rules and the determination of intensity measure for each building via its geographical coordinates and the shakemaps (Michelini et al. 2020).

Then, Sect. 4 deals with the derivation of fragility curves by showing the potential of three different approaches: the first (*empirical* approach) fulfils a direct fitting from post-earthquake data; the others (*empirical-binomial* approach and *heuristic* approach) take advantage of the use of binomial distribution by means of the mean damage value obtained from observational data for each PGA-bin, in one case, and from the vulnerability curve in macroseismic intensity, in the other one. Fragility curves are derived for all the approaches either considering the total sample and also grouping it as a function of construction age and height class.

Finally, in the last section, a comparison between the fragility curves derived for school buildings and those related to the residential building stock (Dolce and Prota 2021; Dolce et al. 2021) is presented in order to provide an insight on the specific aspects differentiating these buildings typologies.

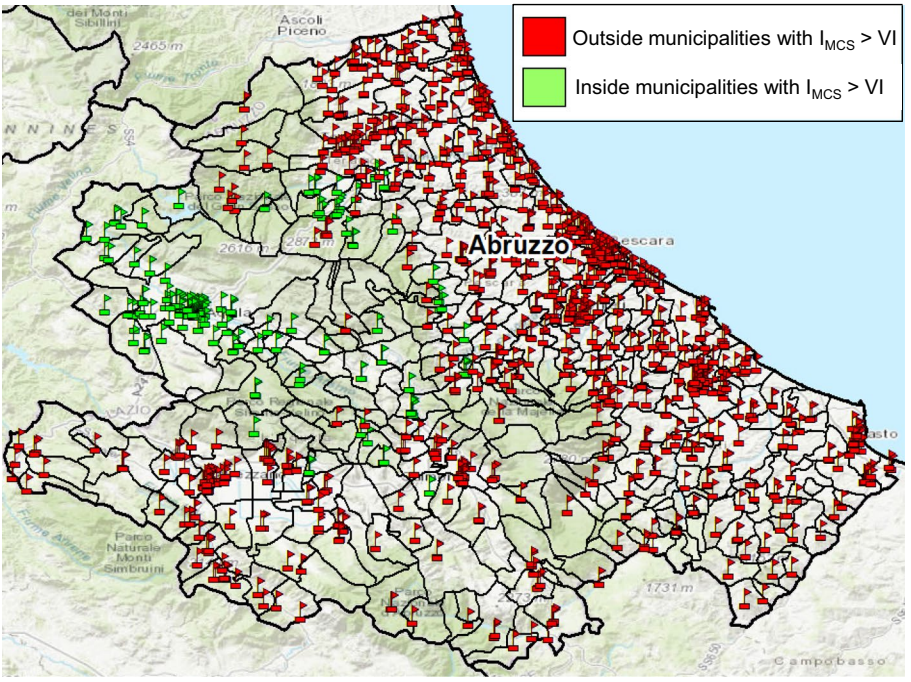

Fig. 1 Location of school buildings in the Abruzzo region

2 Observed damage database of school buildings in the Abruzzo region

The Abruzzo region consists of 4 provinces and 305 municipalities. In the 2004, the registry of the public school buildings of the regional authority (Abruzzo region) counted 1452 schools (see Fig. 1), corresponding to 2229 school buildings, serving a population of about 1.3 million (ISTAT 2011). The 2009 L'Aquila earthquake caused significant damage to school buildings leading to the interruption of teaching activities and relevant socio-economic losses (Dolce et al. 2015).

2.1 The database of school buildings in the Abruzzo region

The aftermath of the L'Aquila 2009 earthquake has been an unique occasion to collect observational data on damage for public and private buildings at regional scale (Dolce and Goretti 2015; Dolce et al. 2019; Di Ludovico et al. 2017). The ReLUIS consortium supported the Italian Department of Civil Protection (DPC) in the usability survey of school buildings by using the AeDES form (Baggio et al. 2007). According to such a form, the damage to structural and non-structural components was classified in terms of severity and extension (as used in §3 to attribute the global damage level to each school building). Moreover, further information on the building characteristics and typologies were also collected. In particular, 481 school buildings were inspected in the area close to the epicenter (belonging to the municipality of L'Aquila and its province with a MCS intensity (Sieberg 1930), I_{MCS}, higher than VI); these data are collected in database B of Table 1. These data, along with other records on school buildings inside and outside the municipalities with $I_{MCS} > VI$, were also included in the Da.D.O. (Dolce et al. 2019) database (named A in the following). It consists of 695 items including the observed damage and building characteristics as well as the geographic coordinates.

Then, in the following months, a massive reconstruction process, mostly funded by the Italian government, interested public and private buildings. It has been managed by the special offices for reconstruction of L'Aquila and other municipalities (i.e. the Special Reconstruction Office of L'Aquila, USRA, and the Special Reconstruction Office of the Crater Municipalities, USRC) that collected and stored all the information on public and private buildings, including damage reports and technical/financial documents. This database (named C in the following) is currently under development since the reconstruction process is still ongoing. Part of these buildings were also hit by the 2016–2017 Central

Table 1 Available database of school buildings in the Abruzzo region

Database	No. schools	No. buildings	Name	Address	Coordinates	Building features	Observed damage
A—Da.D.O (L'Aquila 2009)	–	695	✗	✗	✓	✓	✓
B—ReLUIS 2009	–	481	✓	✓	✗	✓	✓
C—Reconstruction offices	–	156	✓	✓	✓	✓	✓
D—Registry of Abruzzi regional authority	1452	2229	✓	✓	✓	✓	✗

Italy earthquake (Di Ludovico et al. 2019a, b). However, the effect in terms of damage on the as-built or on the retrofitted schools in the post-L'Aquila 2009 buildings is outside of the scope of this study.

To complete the database, the data from the registry of Abruzzo regional authority (named D in the following, made of 2229 items) that dates back to 2004 are also included in the study. It is assumed that these buildings were still used in the 2009. The Registry of Abruzzo regional authority was crucial to have information on school buildings far from the epicentral area, where the damage survey was not made. This information was needed just to get the completeness of the database for low seismic intensity, and therefore small inaccuracies do not affect the results.

Such a large amount of data allowed to have a complete overview of the school buildings of the Abruzzo region that can be employed to derive fragility functions. A summary of the databases selected for this study is reported in Table 1. These four sources of data provide different and complementary information on the school buildings. However, an association of all the items available in each database was needed to have a unique database with all the information needed to derive the fragility curves. This allowed to remove overlapping of the databases and collect only complementary items.

Observed damage were taken from the AeDES forms available in the database A and B and integrated with other data provided by the Reconstruction offices (USRA; USRC) in the form of AeDES forms or damage reports developed by the designer. Damage information on private school building, universities or other buildings not classified as public school were neglected. All the other school buildings available in the regional registry with no information on damage were assumed as undamaged. This results in a database of 2197 items.

In order to assess the robustness of the available dataset, the Completeness Ratio (CR) is used; it is evaluated as the ratio between the number of surveyed school buildings (considering all the typologies, i.e. Reinforced Concrete-RC, masonry-URM and others) and the number school buildings available in the regional registry. This ratio is calculated for each of the 305 municipality of the Abruzzi region. The results in terms of CR are depicted in Fig. 2 in a colour scale for each of the considered dataset (i.e. Database A in Fig. 2a, Database A + B + C in Fig. 2b, Database A + B + C + D in Fig. 2c).

The data on the damaged schools of the ReLUIS 2009 (B) and Reconstruction offices (C) databases are grouped together for sake of simplicity. Note that 37 municipalities have no schools (coloured in white in Fig. 2a). Furthermore, by using the records available in the database A only, some of the municipalities with $I_{MCS} > VI$ have a low CR (i.e. < 0.6).

By integrating these data with damage information available in the databases B and C, most of the buildings in the municipalities with $I_{MCS} > VI$ and in many other municipalities in the province of L'Aquila have $CR > 0.91$ (see Fig. 2b). This led to have complete data on the damaged school at high intensity measures (IMs). However, as clearly showed in Fig. 2b, there is still lack of data on most of the school buildings in the municipalities with $I_{MCS} < VI$, since they were not surveyed. This may result in lack of data (mainly undamaged buildings) at low IMs.

By including all the other items available in the Abruzzi regional registry (D), a $CM > 0.91$ is achieved in all the municipalities of the region (see Fig. 2c).

Out of 2197 school buildings, 1340 schools rely on a RC structure, 697 on a URM structure, 147 on other type of structures (i.e. 126 mixed concrete-masonry structure and 21 steel structure) and for 13 buildings there is no information on the structural system. Due to lack of data for the other typologies (data on damage are available only for 42 and 11

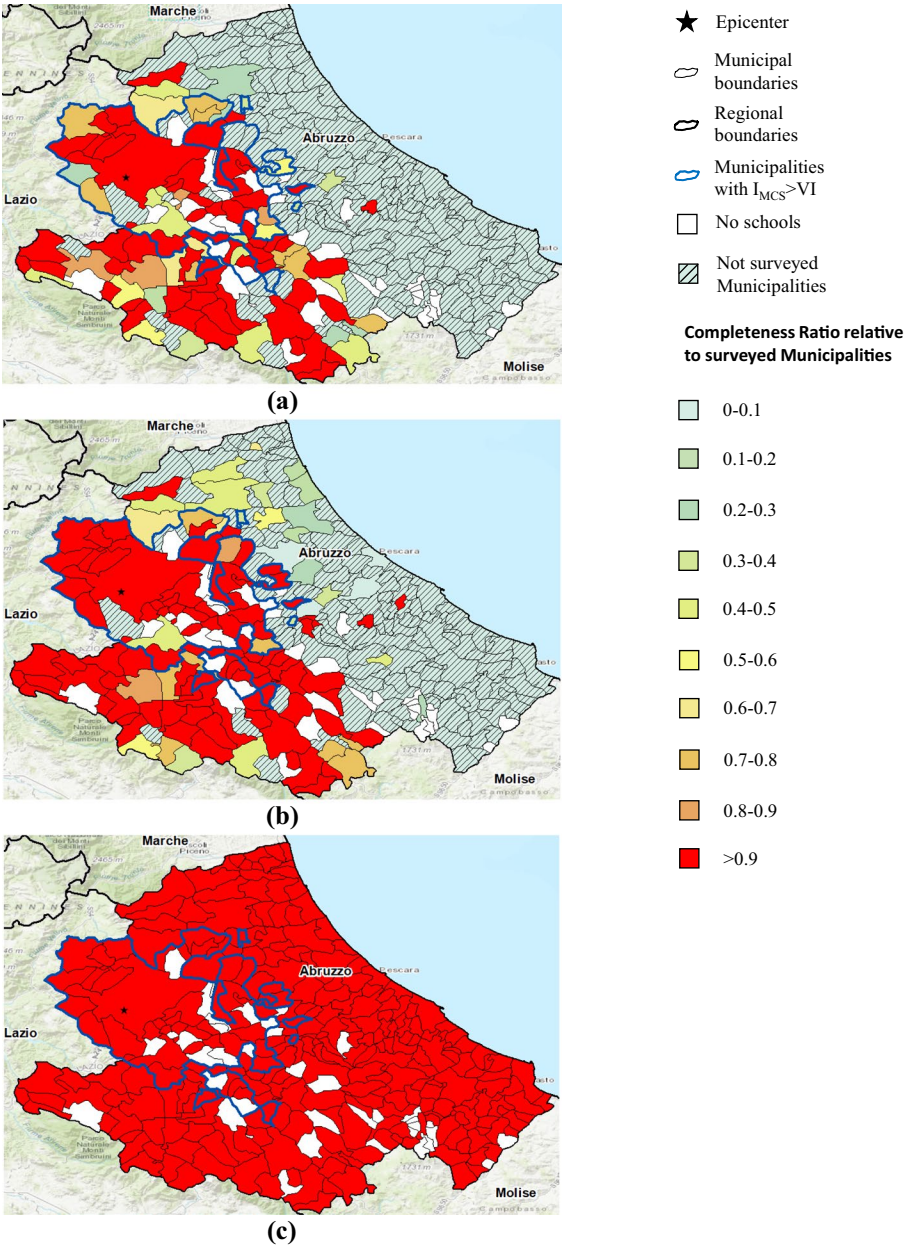

Fig. 2 Spatial distribution of completeness ratio (CR) in the Abruzzo region: Database A (**a**); Database A + B + C; (**c**) Database A + B + C + D

buildings relying on a mixed and steel structural system, respectively), only school buildings relying on RC and URM structures are considered in this study.

Thus, the final dataset used to derive fragility functions consists of 2037 items. It is more than 91% of the total population of school buildings available in the regional registry at the 2004 and it is about the 4.5% of national population of existing school buildings.

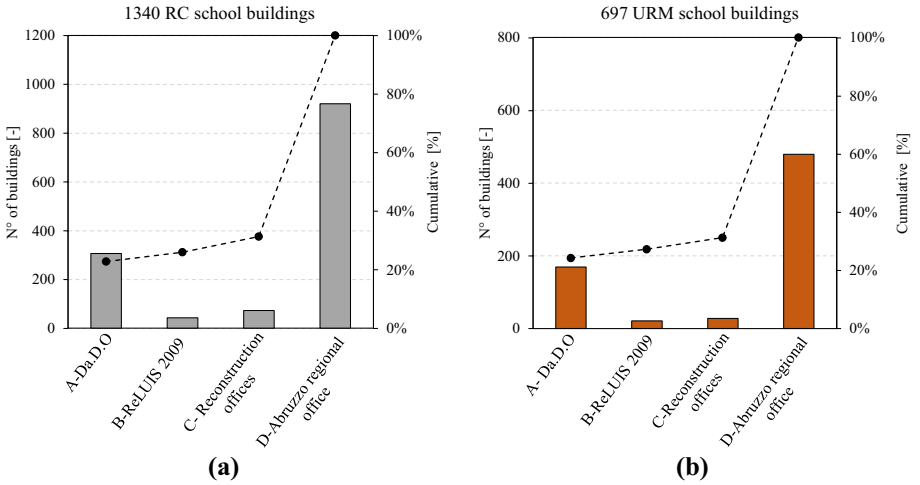

Fig. 3 Distribution of the examined school buildings by database of origin: RC buildings (**a**); URM buildings (**b**)

An overview of the contribution of each database to the total number of RC and URM buildings is reported in Fig. 3. It is worth nothing that most of the buildings (69% both for RC and URM) belong to the regional registry and they do not have any information on damage; thus, in turn, they are assumed as undamaged. The remaining 31% belongs to the A-Da.D.O. database (22% in RC and 24% in URM), to the B-ReLUIS 2009 database (4% in RC and 3% in URM) and to the C-Reconstruction office database (5% RC and 4% in URM).

2.2 Structural features and classification of school buildings

Firstly the main characteristics of the school buildings are analysed in terms of frequency distribution of the construction age, number of storeys above ground and average surface area. The results are depicted in Fig. 4 distinguishing between RC and URM buildings.

Most of the RC buildings were built in the years 1972–1981. About 60% of the RC were built before the 1981 and the remaining part after the 1981. Conversely, as expected, the URM building stock is more ancient that the RC one: about 65% built before 1961. Most of the buildings (about 90%) has one, two or three storeys. The remaining part is populated by buildings with four storeys and only few buildings with five or six storeys. The average surface area of each storey falls within the range 300–650 m^2, for most of the RC buildings, and within the range 300–400 m^2, in the case of URM ones. This is typical of school buildings where a large surface area is preferred to a small one due to architectural and functional needs.

A comparison between the characteristics of school buildings of the Abruzzi region herein analysed and the national ones (with data derived from MIUR (2004) database) is reported in Fig. 5. Due to differences in data content between the two database, the comparison is only related to cumulative distributions of construction age and number of storeys. The figure shows a good agreement between these key factors to determine the

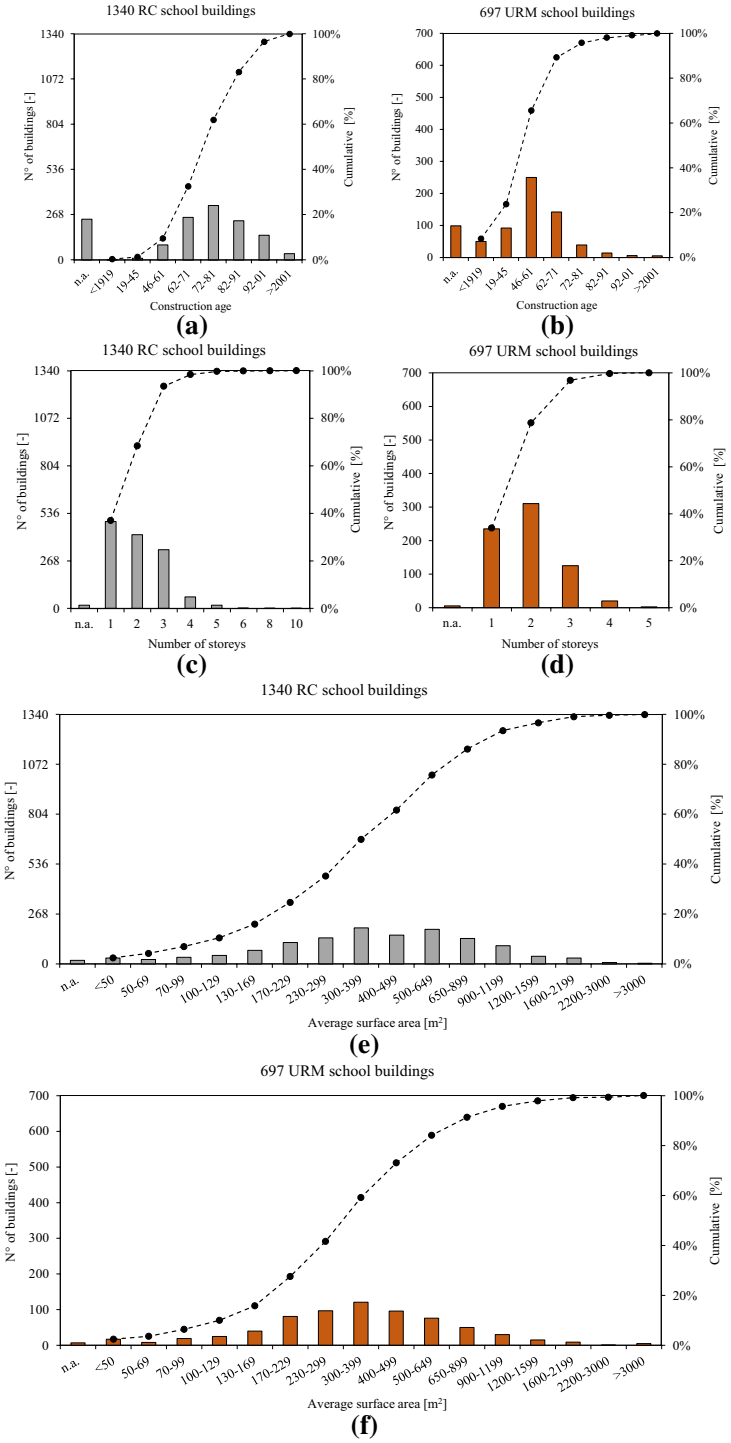

Fig. 4 Characteristics of the RC and URM school buildings in terms of: construction age (**a**, **b**); number of storeys (**c**, **d**); average surface area (**e**, **f**)

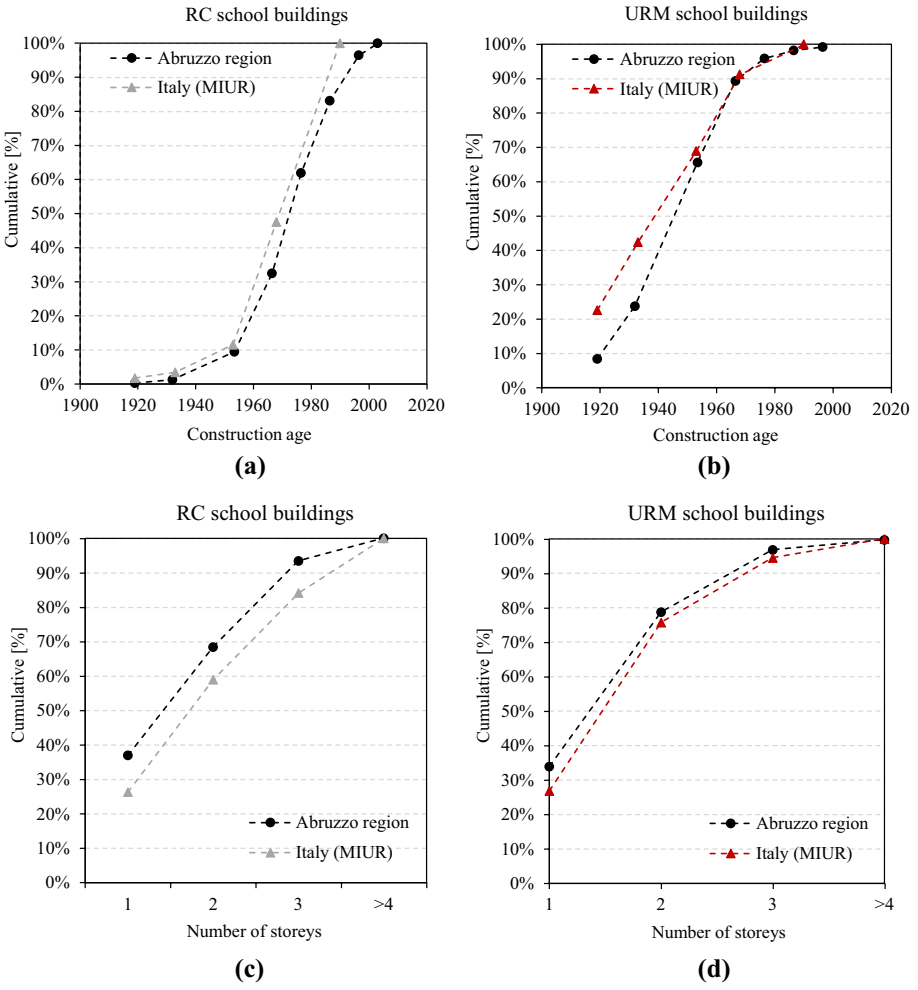

Fig. 5 Comparison between the characteristics of the school buildings of the Abruzzo region database and those available in the MIUR (2004) database at national scale in terms of cumulative distributions of: construction age (**a**, **b**) and number of storeys (**c**, **d**)

buildings' vulnerability, especially in terms of construction age, for RC, and number of stories, for URM school buildings.

With the aim of deriving fragility curves, different groupings have been introduced based on the available data on geometrical-typological characteristics. To this aim, for both structural types, the age and the building height have been adopted as reference. Such factors are typical of seismic risk assessments at large scale (e.g. Dolce et al. 2021), that require the availability of data easily achievable on the whole stock but effective in providing an actual differentiation in the seismic behaviour. To consider a more detailed taxonomy (e.g. by considering also the surface area), and thus increase the number of groupings, was not possible for the examined sample to avoid losing the "minimal" statistical robustness within each grouping.

Concerning the building height, two main classes have been considered, i.e.: low-rise (L) for buildings with one or two storeys; medium-rise (M) for buildings with three or four storeys. The negligible number of school buildings falling in more than four storeys does not allow to develop fragility function for additional height class.

Regarding the construction age, different considerations were made for RC and URM school buildings, respectively. For what concerns RC buildings, the construction age has been used to differentiate the design practices used at the time of construction. In particular, the codes enacted before DM 03/03/1975 can be considered as outdated (note that several municipalities in the Abruzzo region were declared as seismic after the 1915 Avezzano earthquake), providing only a pseudo-constant distribution of horizontal (and vertical) forces to be considered in the seismic design of buildings. On the other hand, DM 03/03/1975 and subsequent codes introduce fundamental innovations in structural analysis and design, explicitly dealing with dissipative aptitude of the structures and capacity design concepts with a systemic approach to the whole building. Thus, even if seismic actions have been considered in the design process before 1980, the division used herein was between RC buildings constructed before (PRE80) and after 1980 (POST80). In previous studies focused on residential buildings (Rosti et al. 2021a,b), the same age of transition was already proven effective in discovering substantial different seismic vulnerability classes. That corroborates the assumption made, being RC structures mostly based on an engineering code-conforming design, despite the unavoidable differences in architectural features of schools and residential buildings. In addition, Fig. 4a highlights that this assumption equally subdivides the original sample. Conversely, for what concerns URM buildings, the design of most of ancient existing buildings is substantially based more on rules of the craft than an engineering-based approach. Consequently, it is difficult to recognize a single emblematic decade or code able to define a clear transition on their seismic behaviour (as also recently confirmed by the data discussed in Del Gaudio et al. 2021). The followed rules of the craft are strongly affected by the level of seismicity and the available materials that may characterize the area under examination. Such rules of the craft comprise many factors able to play a decisive role in defining the actual seismic response of URM buildings, such as: the masonry quality (e.g., roughly classifiable in "regular"- REG or "irregular"—IRREG); the type of diaphragms (e.g. vaults, timber floors, RC slabs, classifiable also as a function of their in-plane shear stiffness); the systematic presence (HQD-high quality details) or lack thereof (LQD-low quality details) of connecting devices (e.g.,

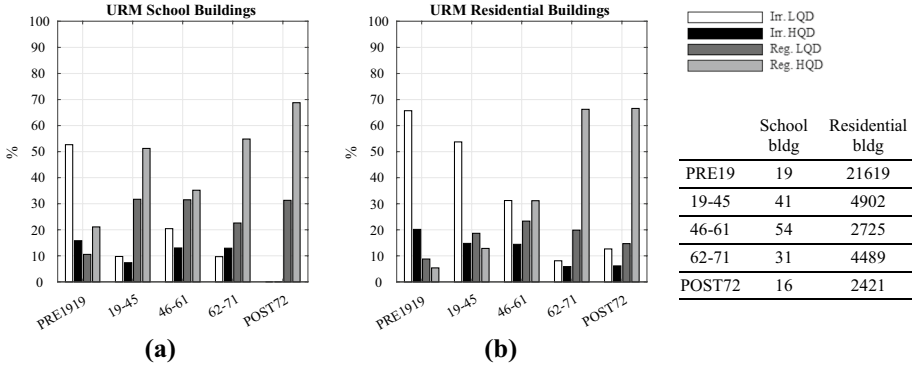

	School bldg	Residential bldg
PRE19	19	21619
19-45	41	4902
46-61	54	2725
62-71	31	4489
POST72	16	2421

Fig. 6 Distribution of the building classes for: URM school buildings (**a**); UMR residential buildings (**b**)

tie rods/tie r.c. beams); the wall-to-wall and wall-to-diaphragms connection. The potential influence of such factors for URM residential buildings was already proven by various studies addressed to derive fragility curves based on observed damage data (e.g. in Del Gaudio et al. 2021; Rosti et al. 2021a,b; Lagomarsino et al. 2021). Given a geographical area, the recurring combinations of such factors in general evolved along the decades together with the progress of the designers' seismic knowledge and, also, the evolution of prescriptions imposed by codes.

To provide an overview on the distribution of building classes for the Abruzzo's URM stock, Fig. 6 compares the data extracted from the AeDES forms collected in Da.D.O. platform referring to both school (Fig. 6a) and residential (Fig. 6b) buildings. The school building stock corresponds to a quite limited number with respect to the overall database considered in this study (only 176 over 697) but still sufficient to establish some trends, whose reliability may be partially confirmed by the more robust dataset of URM residential buildings (in total 36,156). For both, it emerges how there is a progressive trend of increasing in the percentage of regular masonry and HQD along the decades. Moreover, it must be considered that the regular masonry type has changed progressively passing from stone to brick units. According to such concerns, it was decided to consider a number of age classes for URM school buildings higher than the RC ones to verify the possible decrease in the vulnerability with such evolution of structural details. The age classes were thus grouped in PRE45, 46-61, POST61 to have also a quite homogenous number in each set. Although the studies on residential buildings (Del Gaudio et al. 2021; Rosti et al. 2021a,b; Lagomarsino et al. 2021) highlighted an appreciable difference in the fragility curves passing from PRE19 to 19–45 age, for the stock under examination the number of school buildings dated back before 1919 was too low to guarantee a robust statistical analysis. Indeed, it is significantly lower than those built in 19–45 (differently from the residential stock as depicted in Fig. 5). Thisis consistent with the fact that the '20 s largely coincide with the schooling phase in Italy.

Figure 7 depicts the distribution of the sample in the outlined groups, i.e.: PRE80-L, POST80-L, PRE80-M, POST80-M, for the RC school buildings (Fig. 7a); and PRE45-L, PRE45-M, 46–61-L, 46–61-M, POST61-L, POST61-M, for the URM school buildings

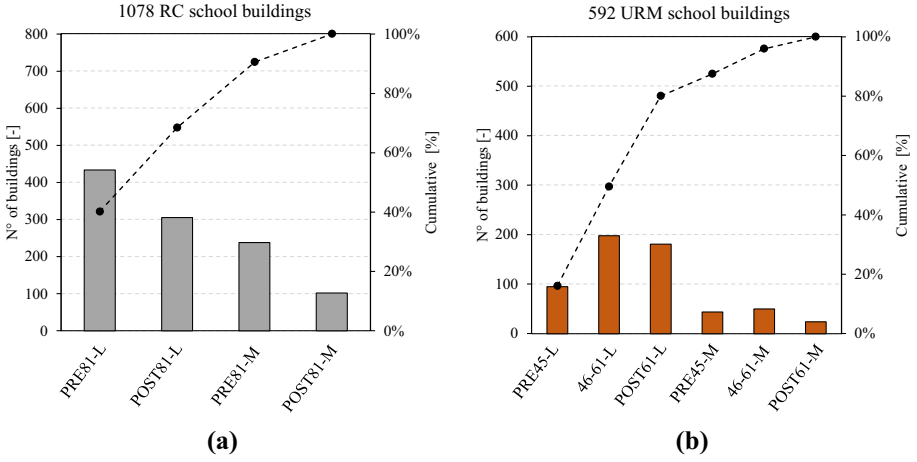

Fig. 7 Distribution of the adopted groupings for: RC school buildings (**a**); URM school buildings (**b**)

(Fig. 7b). Note that the total number of buildings adopted is slightly lower than that analyzed in Fig. 4. In fact, about the 30% and 18% of the available RC and URM school buildings, respectively, do not have information on the number of storey or construction age, thus making their classification not feasible.

3 Empirical damage probability matrices

The preliminary step for the derivation of the fragility curves is to organise the damage data according to bins of increasing ground motion levels to obtain Damage Probability Matrices (DPM). The organisation of the data consists of two main steps: (i) the assignment of the damage grade to each individual school building according to the European Macroseismic Scale (EMS-98, Grünthal et al. 1998) and (ii) the assignment of the corresponding Peak Ground Acceleration (PGA) value that hit the building. ShakeMaps are needed to complement direct measurements of ground motion from recording stations, as measurements are not available for every single building.

The ShakeMaps adopted in this work follow the methodology reported in (Michelini et al. 2020). It starts with the definition of a grid and a calculation based on Ground Motion Prediction Equations (GMPEs), conditioned on the real measurements (i.e. INGV broadband and the Italian Strong Motion Network—Rete Accelerometrica Nazionale). The grid corresponds with the station locations and with a uniformly spaced mesh far away from the epicenter. The intensity values are modified to incorporate site effects, evaluated with a nationwide 1:100,000 geological map calibrated against the average shear wave velocity of the top 30 m of the subsurface profile (VS_{30}).

Figure 8a shows the ShakeMaps in terms of PGA of the 6th April 2009 L'Aquila earthquake, which characterizes the ground motion for the majority of the investigated buildings. In particular, for each georeferenced building, the value of PGA is determined as the maximum value among those of the mainshock and of the relevant aftershocks (i.e.

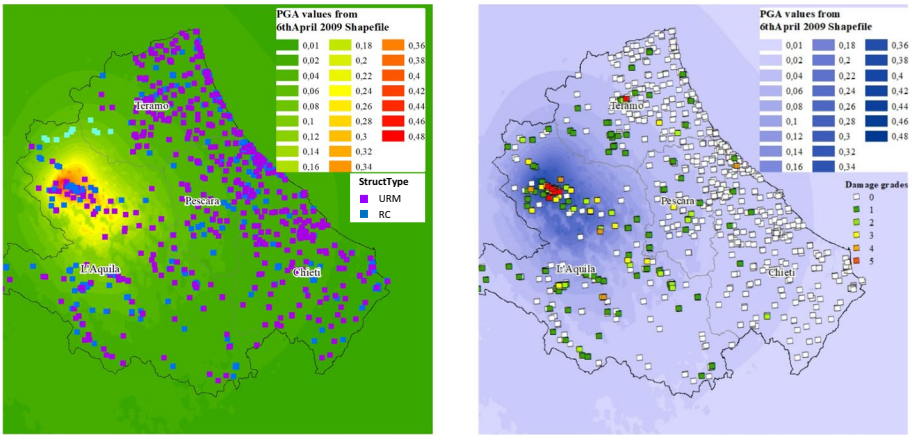

(a) **(b)**

Fig. 8 Shakemaps of 6th April 2009 Earthquake from shapefiles (Michelini et al. 2020). School buildings indicated by light blue color are those for which the maximum PGA was attained in an aftershock (**a**); EMS-98 damage grades assigned to each school building (**b**)

7th of April 2009 Mw 4.8, 7th of April 2009 Mw 5.3, 9th of April 2009 Mw 5.1, 9th of April 2009 Mw 4.9 Earthquakes) at the site location. Figure 8a also reports the spatial representation of school buildings herein investigated. Note that the maximum PGA values correspond to the 9th of April 2009 aftershocks instead of mainshock only for very few buildings (highlighted with light blue colour in the figure). This is due to the migration of seismicity to the northern area (Chiarabba et al. 2009).

Fragility curves estimation requires damage characterization in terms of damage grades for the whole building. By contrast, damage survey forms, commonly adopted in Italy in the post-earthquake emergency phase, collect damage information for single building components with the aim of assigning a usability rating rather than a global damage grade. Thus, damage conversion rules must be introduced to establish an association between these two scales (i.e. global at building level and local at component level) and provide a proper conversion. For what concerns the global damage state, in this work, reference is made to the five damage states introduced by the EMS-98 (Grünthal et al. 1998), which provides, for each damage state, a description of the expected damage and extension on the building, differentiated for RC and URM buildings. Figure 8b shows the damage grade assigned to each school building.

The EMS-98 classification schemes also represented a benchmark for the damage classification of the AeDES inspection forms (Baggio et al. 2007), a valuable source for the database definition in this work (see Sect. 2). In particular, "Sect. 4—Damage to the structural components" of the AeDES form identifies four damage states (D0-no damage, D1, slight damage; D2-D3 medium-severe damage; D4-D5 very heavy damage or collapse) and three levels of extent ($< 1/3$; 1/3–2/3; $> 2/3$) differentiated for structural and non-structural components (i.e. vertical structures, floors, stairs, roofs and infills/partitions).

Damage conversion rules may mainly follow two different approaches:

- An integral approach that considers an average damage weighted on the extent level and on various components. According to such an approach, it is possible to refer only to specific components (e.g. the vertical ones, eventually integrated by infills/partitions in the case of RC buildings) or to consider almost the whole set (i.e. by including also diaphragms, roof and, possibly, also stairs). The damage so computed is a real number ranging from 0 to 5 that requires to be discretized in order then to be converted to the EMS-98 damage grades. Proposals available in the literature that follow this approach are those of (Zucconi et al. 2017; De Martino et al. 2017; Lagomarsino et al. 2021).
- A peak approach that considers the maximum damage level attained on selected (one or more) components. The criteria adopted for the conversion may also account for the damage extent. The method allows to directly define a discrete global EMS-98 damage grade. Proposals belonging to this approach are those of (Braga et al. 1982; Rota et al. 2008; Dolce et al. 2019; Del Gaudio et al. 2017, 2020; Rosti et al. 2021a, b).

In this work, a peak approach is adopted for both RC and URM school buildings according to the criteria summarized in Fig. 9 to convert the information collected in the AeDES forms into the EMS-98 Damage States (DSk, $k = 0 \ldots 5$). This is because such an approach has proven to be better correlated with the usability rating outcomes, as documented in the following, while the integral approach should be more consistent with the evaluation of economic losses.

The conversion scheme adopted for RC buildings follows the proposal of Del Gaudio et al. (2017) and Rosti et al. (2018); they consider the maximum damage states attained by vertical structures and infills/partitions. The latter are considered only for the first three

EMS-98	RC buildings		URM buildings	
	Vertical structures	Infills/partitions	Peak damage	Secondary damage
DS0	D0	D0	D0	
DS1	D1 - <1/3 D1 - 1/3-2/3 D1 - >2/3	D1 - <1/3 D1 - 1/3-2/3 D1 - >2/3	D1- <1/3 D1 - 1/3-2/3 D1- >2/3 D2-D3 - <1/3	D1 =0
DS2	D2-D3 - <1/3	D2-D3 - <1/3 D2-D3 - 1/3-2/3 D2-D3 - >2/3	D2-D3 - <1/3 D2-D3 - 1/3-2/3	D1 >0
DS3	D2-D3 - 1/3-2/3 D2-D3 - >2/3	D4-D5 - <1/3 D4-D5 - 1/3-2/3 D4-D5 - >2/3	D2-D3 - >2/3 D4-D5 - <1/3	D2-D3 <1/3
DS4	D4-D5 - <1/3 D4-D5 - 1/3-2/3		D4-D5 - <1/3 D4-D5 - 1/3-2/3	D2-D3 ≥1/3
DS5	D4-D5 - >2/3		D4-D5 - >2/3	

Fig. 9 Conversion rules adopted to associate the data collected in the AeDES survey forms into discrete EMS-98 Damage States

damage states, and the worst damage between vertical structures and infills/partition is assumed as reference. The choice of including also the response of infills/partitions recognizes their strong impact on damage estimation and resulting losses, as highlighted by recent studies (e.g. Dolce and Goretti 2015; Del Vecchio et al. 2020).

For what concerns URM school buildings, the conversion scheme starts from the proposal of Dolce et al. (2019) by introducing in this work slight modifications that are mainly related to some reinterpretations of the linguistic descriptions of EMS-98. These reinterpretations are addressed to solve some irregularities noticed by applying the proposal of Dolce et al. (2019) (e.g., it gives damage probability matrices with a very low number of DS2, compared to DS1 and DS3, and an almost equal number of DS4 and DS5). Note that, for a given grade, definitions of EMS-98 mainly refer to the description of cracks associated with the damage peak. Thus, considering that cracks of various severity may be present together (and the same applies for the rules adopted for properly filling in the AeDES form), a complete conversion rule requires to consider both the peak damage but also the secondary one (i.e. the one associated with a severity lower than peak one). For the sake of clarity, as an example, DS1 is when D2–D3 is "$<1/3$" but D1 is not present in the building, while DS2 is assigned to the whole building when D2–D3 is again "$<1/3$" but also D1 was observed is other parts of the building ("$<1/3$" or "1/3–2/3", synthetically indicated in Fig. 9 as "D1 > 0"). Moreover, reference is herein made only to vertical walls. That appears justifiable by considering that: school buildings are mostly characterized by rigid diaphragms (see Sect. 2) and statistical analyses reported in Cattari and Angiolilli (2022), carried out on the data collected in Da.D.O. platform on URM residential buildings hit by L'Aquila 2009 earthquake, highlighted that, in case of rigid diaphragms, the highest damage level is always associated with walls (differently from the case in which vaults or flexible floors are present).

Figure 10 depicts the resulting empirical DPM for the stock of RC (Fig. 9a) and URM (Fig. 9b) school buildings herein analysed (i.e. "all" 1340 and 690 RC and UMR buildings). The ground motion range, expressed in terms of PGA, was subdivided into equally-spaced bins of 0.06 g. In general, a quite regular progression in the increasing percentage

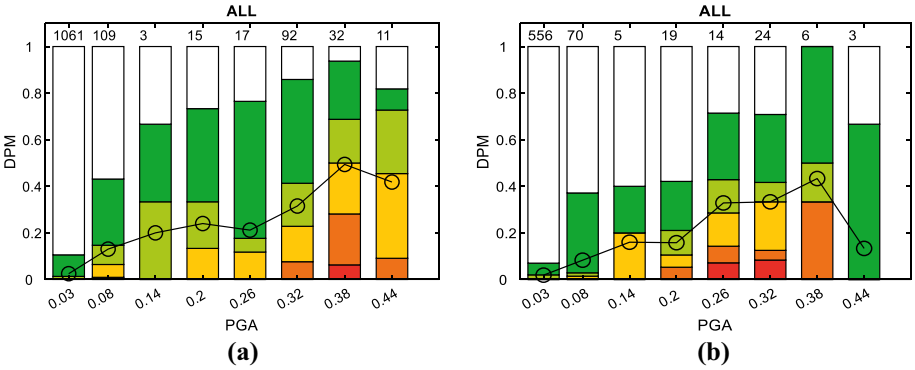

Fig. 10 Empirical Damage Probability Matrix (DPM) for RC (**a**) and URM (**b**) school buildings. For each bin: damage grades are indicated using colors of Fig. 9, the number of school buildings is indicated at the top of each column, while the mean damage (Eq. 4) is indicated by the black circle (the black line shows the increase of damage with the PGA)

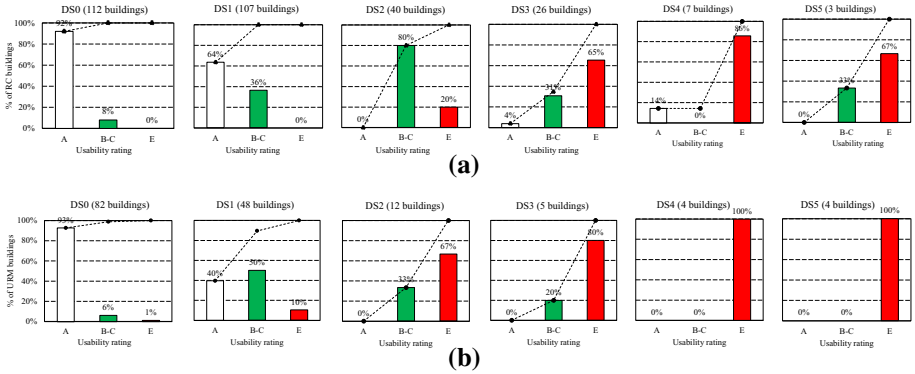

Fig. 11 Distribution of the usability rating as function of the damage state for RC (**a**) and URM school buildings (**b**)

of higher damage states together with the increase of seismic input may be noticed. The unexpected trend shown by last bins is substantially ascribable to their lower robustness from the statistical point of view.

Finally, Fig. 11 reports, for the sub-set of school buildings comprised in database A of Sect. 2, the usability rating percentages associated with each damage state. In particular, according to the AeDES, the tags A, B, C, E correspond respectively to: usable building; to building usable only after short term countermeasures; to partially usable building; and to unusable building. As expected, Fig. 11 shows that the percentage of B–C and E rating progressively increases with the damage state. In the case of URM school buildings, a more significant percentage of E rating appears since DS2. This is because for URM school buildings, the cracks producing the attainment of DS2 involve structural components, while in the case of RC school buildings they are mainly related to non-structural elements (infills/partitions) that may be more easily repaired (thus leading to B/C usability rating attribution).

4 Derivation of fragility curves

4.1 Basics of the adopted approaches

The statistical model selected to represent the relationship between the ground motion intensity measure and the probability of exceeding the damage grades is the cumulative lognormal distribution. The choice of the most appropriate intensity measure is a critical issue largely investigated in the literature (e.g. Baker and Cornell 2005; Luco and Cornell 2007; Minas and Galasso 2019; Kita et al. 2020). In this work, the PGA has been adopted as intensity measure. That appears a reasonable choice for URM buildings since reference periods are usually small and fall within the range in which there is a significant record-to-record variability, also considering spectral values. In the case of RC buildings, the spectral value associated to the fundamental period would be more efficient, but it is worth noting that the RC school building stock is mainly formed by low rise buildings, with rather small characteristic periods.

According to this model, only two parameters are necessary to describe the fragility curve associated with the given DSk (k = 1,.0.5): the median value of the intensity measure that induces a damage equal or greater than DSk (PGA_{DSk}) and the corresponding dispersion β_{DSk}, which depends on the record-to-record variability and the inhomogeneity of buildings in the same class. This model is worldwide used for seismic risk analyses (HAZUS 1999; Rossetto et al. 2014; Silva et al. 2019, 2020; Baraschino et al. 2020; Spence et al. 2021) and is also coherent with the framework issued by the Italian Civil Protection Department in 2018 for the most recent National Risk Assessment (NRA 2018) in Italy (Dolce and Prota 2021; Dolce et al. 2021).

In this paper, three different approaches are used to derive fragility curves taking advantage of the post-earthquake damage data presented in Sect. 2:

- a direct *empirical approach* where an optimization procedure is directly applied to observational data allowing to obtain the unknown parameters;
- a hybrid approach (named *empirical-binomial approach*) that exploits the simulated damage probability matrix by means of probability density functions, ensuring a regular distribution (i.e. binomial) of damage states, derived from the mean damage μ_D evaluated from the counts of buildings suffering the observed damage states;
- a *heuristic approach* based on the expertise that is implicit in the EMS-98 scale, which assumes a regular increase of mean damage with the earthquake intensity (vulnerability curves derived with fuzzy assumptions on the binomial damage distribution—Lagomarsino and Giovinazzi 2006), directly fitted on the available post-earthquake damage data.

Details on each of these three methods are provided in the following.

4.1.1 The empirical approach

Fragility curves obtained by the empirical approach are obtained by fitting the assumed statistical model to observational data. For comparability purposes, this approach is quite similar to that adopted within the ICPD 2018 framework for residential buildings (Del Gaudio et al. 2020; Rosti et al. 2021a, b). The parameters of the fragility curves are herein

estimated by maximizing the likelihood function (Maximum Likelihood Estimation-MLE, e.g. Baker and cornell 2015) via an optimization algorithm, where the counts of buildings suffering a given damage grade belonging to the *i*th-PGA bin is assumed to follow a multinomial distribution (Charvet et al. 2014):

$$L\left(n_{i,DS},P_{i,DS}\right) = \prod_{DS=0}^{5}\prod_{i=1}^{m}\frac{N_i!}{n_{i,DS}!}P_{i,DS}^{n_{i,DS}} \tag{1}$$

where, for the ith-bin: $n_{i,DS}$ is the number of buildings suffering a given DS, N_i is the total number of buildings ($N_i = \sum_{DS} n_{i,DS}$) and $P_{i,DS}$ represents the conditional probability of suffering a given DS. This probability is herein evaluated as a function of lognormal cumulative function:

$$P_{i,DS} = \begin{cases} 1 - \text{logncdf}(PGA_i, \lambda_{DS+1}, \beta) & DS = 0 \\ \text{logncdf}(PGA_i, \lambda_{DS}, \beta) - \text{logncdf}(PGA_i, \lambda_{DS+1}, \beta) & 1 \le DS < 5 \\ \text{logncdf}(PGA_i, \lambda_{DS}, \beta) & DS = 5 \end{cases} \tag{2}$$

The above optimization procedure is set to simultaneously fit all the 5 fragility curves for a given building class to observational data assuming a common value for logarithmic standard deviation β (dispersion) for all DSk and different values of logarithmic mean λ_{DS} (where $PGA_{DSk} = \exp(\lambda_{DS})$).

4.1.2 The empirical-binomial approach

The use of the empirical-binomial approach is addressed to partially solve the irregularity and sparseness of observational damage data shown in DPM of Fig. 10. Indeed, studies have shown that observational damage frequencies are well reproduced by a binomial probability density function (Braga et al. 1982; Sabetta et al. 1998; Lagomarsino and Giovanazzi 2006; Rosti et al. 2018; Lagomarsino et al. 2021) or a beta probability density function (Giovinazzi and Lagomarsino 2005; Lallemant et al. 2015; Rosti et al. 2020).

In this paper the binomial distribution has been assumed, then the term $n_{I,DS}$ of Eq. 1 could be substituted by the following:

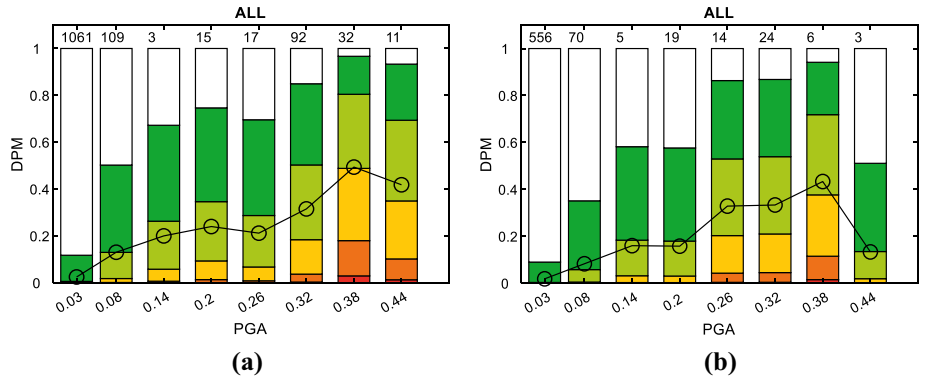

Fig. 12 DPM for RC (**a**) and URM (**b**) school buildings adopted for deriving the fragility curves with the empirical-binomial approach

$$\widetilde{I} = \frac{5!}{DS!(5-DS)!}\mu_D^{DS}\left(1-\mu_{D,i}\right)^{5-DS} \tag{3}$$

where

$$\mu_{D,i} = \frac{\sum_{DS}\left(I_{i,DS}\cdot DS\right)}{5\sum_{DS}I_{i,DS}} \tag{4}$$

represents the mean damage evaluated for observed damage data in the ith-PGA bin.

The updated DPMs adopted for the fitting are those illustrated in Fig. 12. It is worth noting that considering altogether the RC or the URM school buildings, the DS distribution is more disperse than the binomial distribution, because buildings of different age and height are grouped. This is the reason why, by comparing Figs. 10 and 12 it seems that the empirical-binomial approach eliminates a large part of the higher and lower levels of damage. However, the application of this approach to specific groupings, as it will be made in the Sect. 4.2, has shown that the binomial distribution fits very well the observed damage.

4.1.3 The heuristic approach

The third method (classified as *heuristic*) aims at guaranteeing a fairly good fit of the actual damage data while at the same time ensuring physically consistent results for both low and high values of the seismic intensity (for which observed data are incomplete or lacking). This approach starts from the original proposal of Lagomarsino and Giovinazzi (2006) but it has been recently further developed by Lagomarsino et al. (2021) thanks to the valuable calibration supported by the use of data on URM residential buildings collected in Da.D.O. platform (Dolce et al. 2019).

According to this approach, the fitting of observed damage data is carried out in the domain given by the mean damage grade (μ_D) and the macroseismic intensity (I) with the aim of deriving the free parameters (V and Q) of the macroseismic vulnerability curve expressed by the following:

$$\mu_D = 2.5\left[1+\tanh\left(\frac{I+6.25V-Q-10.8}{Q}\right)\right] \tag{5}$$

where V is the vulnerability index and Q the ductility index. It is worth noting that, differently from the application to URM residential buildings made in Lagomarsino et al. (2021), the two parameters have been here kept independent in order to better fit the behaviour of URM and RC buildings of different ages and height.

Although for each school building the macroseismic intensity in the village/town is known, PGA is used as intensity measure also for the heuristic approach, in order to avoid the introduction of an additional dispersion/noise in the fragility curves. Indeed, PGA from shakemap is definitely more reliable and accurate as intensity measure for each single buildings, because the macroseismic intensity is defined at urban scale, thus losing the spatial variation that is caught by the shakemap, in particular due to local soil conditions.

Therefore, for each bin of values of PGA, it is necessary converting the central value of PGA into macroseismic intensity I, by adopting a I-PGA correlation law. However, the adoption of such law is only functional to operate the fitting in the domain coherent with Eq. (5), but it doesn't alter the numerical consistence of each bin; indeed, the conversion has been operated by referring to the central value of each bin. The same correlation has

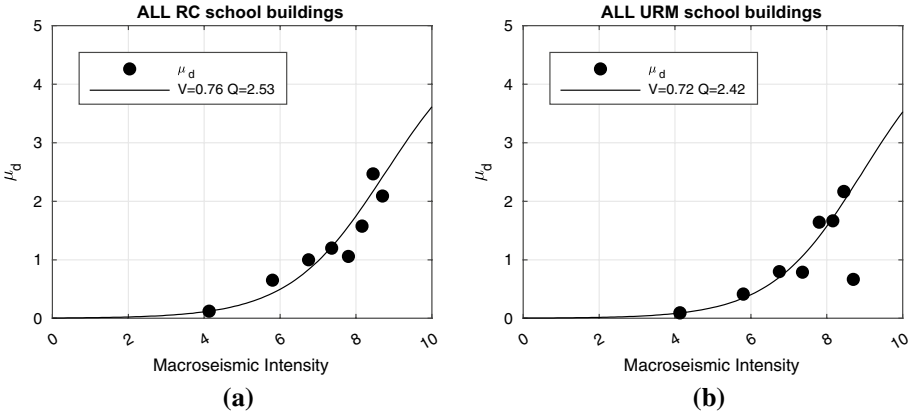

Fig. 13 Vulnerability curves fitted by the observed damage data on: **a** URM school buildings; **b** RC school buildings

been then applied to come back in the PGA domain; therefore, the final result is not sensitive to the choice of the I-PGA correlation law.

In particular, the following relationship has been adopted: $PGA = c_1 c_2^{I-5}$, where c_1 represents the PGA for intensity I = 5, while c_2 is the factor of increase of PGA due to an increase of 1 of the macroseismic intensity. In this work, c_1 and c_2 have been assumed equal to 0.047 and 1.7, respectively.

According to the original macroseismic method proposed in Lagomarsino and Giovinazzi (2006), Eq. (5) assumes that the completion of DPMs is made according to the binomial probability distribution.

The fitted points and the resulting V and Q values obtained by considering the whole sample of URM and RC schools are illustrated in Fig. 13. Once the V and Q values are fitted, according to the procedure described in Lagomarsino et al. (2021), it is possible to convert the vulnerability curve into the corresponding fragility curve.

The mean damage of the binomial distribution that corresponds to a probability of exceeding each DSk of 50% is given by:

$$\mu_{D,k} = 0.9k - 0.2 \ \ (k = 1, .., 5) \tag{6}$$

Therefore, fragility curves in terms of PGA should be obtained numerically from Eqs. (5) and (6), but they would not result a lognormal function; however, the shape is very near to a lognormal cumulative distribution, defined by the two parameters: PGA_{DSk} and β_{DSk}. In particular, the mean value of the PGA for each DS is provided analytically as follows:

$$PGA_{DSk}(V, k) = c_1 c_2^{(I_{Dk}-5)} = c_1 c_2^{[10.8-6.25V+Q[1+atanh(0.36k-1.08)]]} \tag{7}$$

The dispersion β, assumed as constant for all DSk, depends only by the parameter Q, as well as by the I-PGA correlation law (c_1 and c_2).

Figure 14 represents the DPMs obtained after the fitting of the vulnerability curve. It is worth noting that the heuristic approach includes a further assumption with respect to the empirical-binomial approach. Indeed, in addition to the binomial distribution for any bin, the heuristic approach assumes an a-priori gradual increase of the mean damage with the intensity measure, ruled by Eq. (5) with two free parameters (V and Q). This is useful

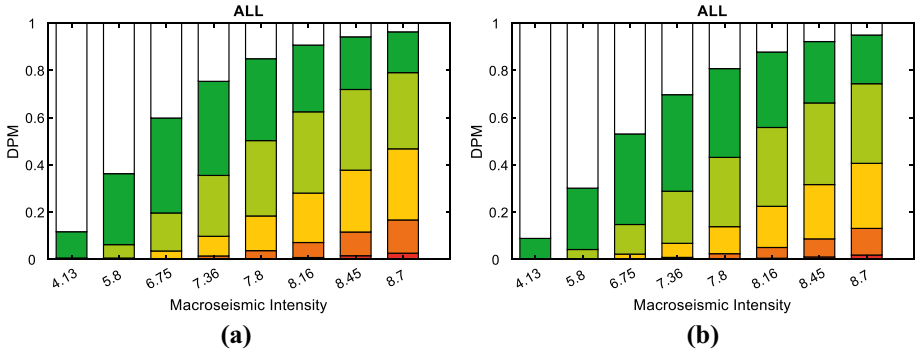

Fig. 14 DPM for RC (**a**) and URM (**b**) school buildings obtained from the vulnerability curve of the heuristic approach

when data are sparse and/or errors or bias are expected in the filling out of the damage forms. The final DPMs look smoother than what directly observed, but it should be considered that: (1) due to the limited number of buildings in the bins with higher PGA (in particular for URM buildings), the cases with DS5 may be outlier; (2) empirical DPMs in Fig. 10 are referred to the whole database of RC or URM buildings, thus including structures with very different vulnerability.

4.2 Fragility curves for RC school buildings

This section presents the fragility curves of RC school buildings obtained using the three approaches described in the previous section.

Figures 15 and 16 show the resulting curves for the whole stock and the groupings, respectively; they also report the total number of schools for each group. Note that the empirical probabilities reported in Figs. 15 and 16 are those obtained using observational data (see Fig. 10).

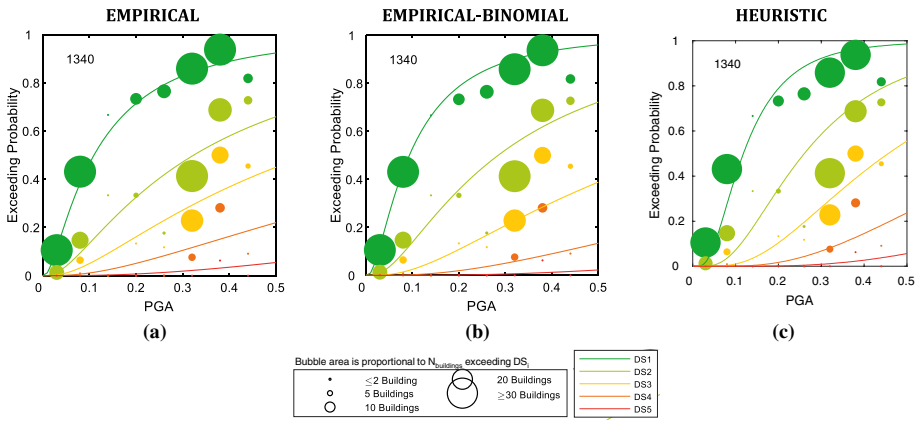

Fig. 15 Fragility curves for RC school buildings derived on the whole stock via the empirical (**a**), empirical-binomial (**b**) and heuristic (**c**) approaches, respectively

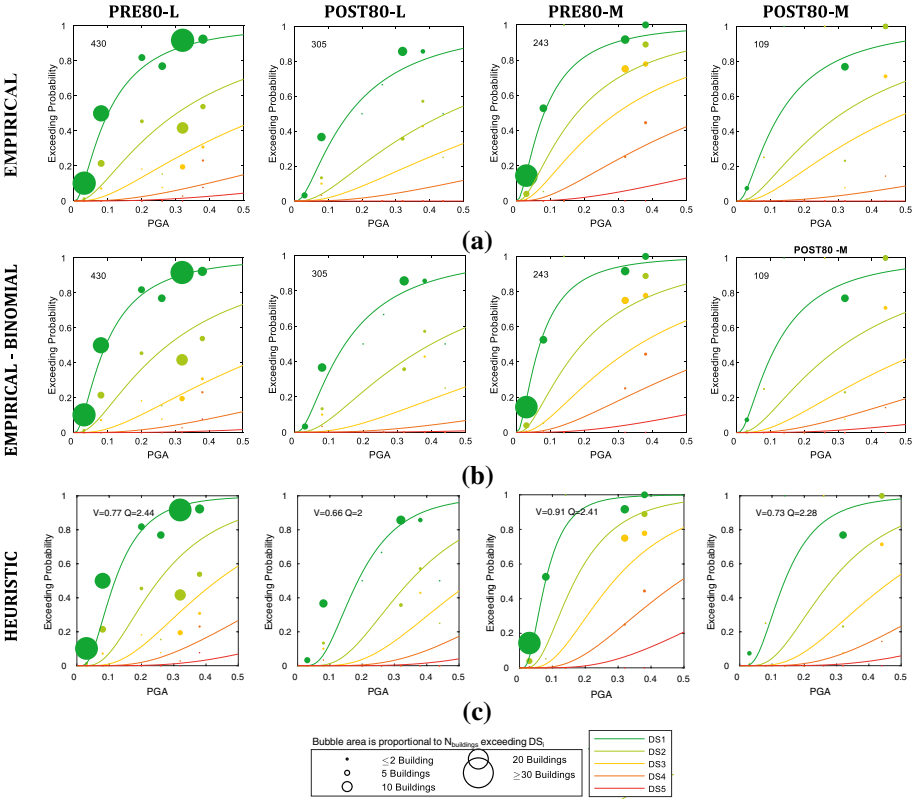

Fig. 16 Fragility curves for RC school buildings (groupings PRE80-L, POST80-L, PRE80-M, POST80-M): empirical (**a**), empirical-binomial (**b**) and heuristic approach(**c**)

Table 2 RC school buildings: median PGA (PGA_{DSk}, with k = 1…5), and dispersion β)

Approch	Group	PGA_{DS1}	PGA_{DS2}	PGA_{DS3}	PGA_{DS4}	PGA_{DS5}	β
Empirical	ALL	0.11	0.32	0.57	1.13	2.73	1.06
	PRE80-L	0.10	0.30	0.59	1.39	2.66	0.98
	POST80-L	0.16	0.45	0.77	1.60	–	0.98
	PRE80-M	0.08	0.18	0.30	0.61	1.52	0.98
	POST80-M	0.13	0.31	0.50	1.91	–	0.98
Empirical-binomial	ALL	0.09	0.28	0.66	1.45	3.42	0.96
	PRE80-L	0.09	0.28	0.66	1.51	3.67	0.94
	POST80-L	0.15	0.40	0.92	2.06	4.83	0.94
	PRE80-M	0.07	0.19	0.36	0.71	1.66	0.94
	POST80-M	0.12	0.31	0.60	1.13	2.43	0.94
Heuristic	ALL	0.12	0.26	0.46	0.80	1.41	0.66
	PRE80-L	0.12	0.25	0.43	0.75	1.29	0.64
	POST80-L	0.19	0.35	0.54	0.85	1.33	0.56
	PRE80-M	0.08	0.17	0.29	0.49	0.84	0.63
	POST80-M	0.14	0.28	0.47	0.78	1.30	0.61

The fragility curves obtained by using the three approaches are in good accordance with empirical probabilities both for the whole stock of schools and the proposed groupings. For the heuristic approach, Fig. 16 also reports the values of V and Q resulting from the fitting of the vulnerability curve.

Table 2 summarizes the values of the two parameters that identify each fragility curve. For all the three methods, within the same grouping, the fitting has been carried out by assuming a constant value of the dispersion in all cases. In the case of the pure empirical approach, for the derivation of curves associated with DS5 of the POST80 grouping the empirical data are statistically not sufficient to fit the parameters of the fragility curves (this problem is overcome by the other two approaches, thanks to the use of the binomial distribution to complete the missing data).

Table 2 shows that in general the median values of PGA_{DSk} obtained from the empirical and empirical-binomial approaches are higher than those from the heuristic one. Moreover, the dispersion values β associated with the empirical and empirical-binominal approaches (0.98 and 0.94, respectively) and higher than those associated with the heuristic one. Therefore, the heuristic approach appears to be more fragile, in terms of median values, but less disperse than the empirical and empirical-binomial ones.

Regarding the dispersion, the three approaches account for the same sources of the uncertainty: the seismic input, the inter and intra buildings variability, and, finally, the epistemic uncertainty possibly resulting from a subjectivity degree of surveyors in attributing the damage rating in the AeDES form (although strongly reduced in last Italian earthquakes thanks to the valuable effort of Italian Department of Civil Protection in increasing the training of surveyors). Therefore, the reasons of such differences in the β values are due to the differences in the hypotheses on which the methods are based. In particular, it is useful recalling that the heuristic model assumes a regular trend of μ_D with IM (i.e.by fitting the observed damage data as a function of macroseismic intensity), with a rate of increase (ruled by the parameter Q) that cannot be too flat (Fig. 13) and a direct derivation of fragility curves by means of the binomial damage distribution. Conversely, the pure empirical approach relies completely on observed data, that are more irregular and disperse. Finally, the use of the binomial distribution in the empirical-binomial approach (applied separately to each empirical μ_D computed in each PGA-bin) slightly reduces the dispersion with respect to the pure empirical one.

The fragility curves evaluated by means of the three approaches show a clear and appropriate hierarchy with the construction age and the number of storeys as depicted in Fig. 17, where the curves are grouped (PRE80-L, POST80-L, PRE80-M, POST80-M) for each damage state. It is worth noting that only the first three DSs are represented because they are more significant in the range of interest of the PGA (these curves are represented in Fig. 16 while the corresponding parameters are in Table 2). In particular, for each DS: (1) given the building height, the fragility decreases with the construction age (passing from PRE-80 to POST-80), consistently with the design evolution compliant to seismic codes; (2) given the construction age, the fragility increases as the height of the building increases (passing from L to M).

4.3 Fragility curves for URM school buildings

In this section, the fragility curves of URM school buildings are presented by using the same format adopted for RC school buildings.

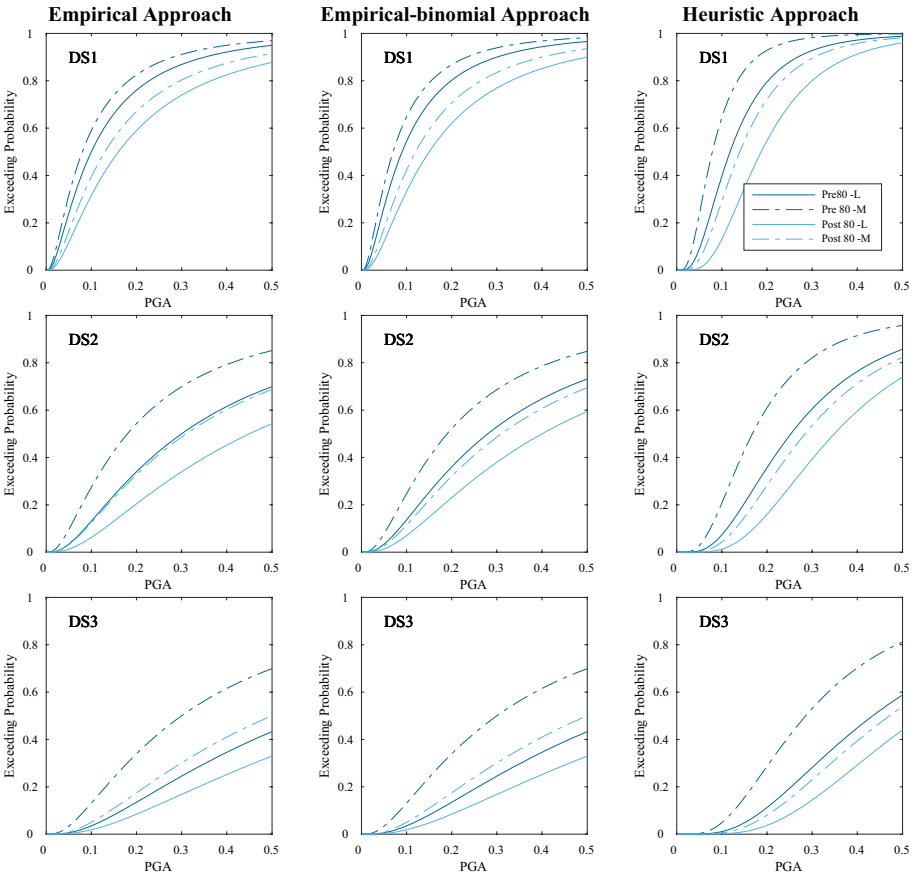

Fig. 17 Comparison of the seismic fragility, for the first three damage states, captured by three adopted approaches on the adopted classes (PRE80-L, POST80-L, PRE80-M, POST80-M)

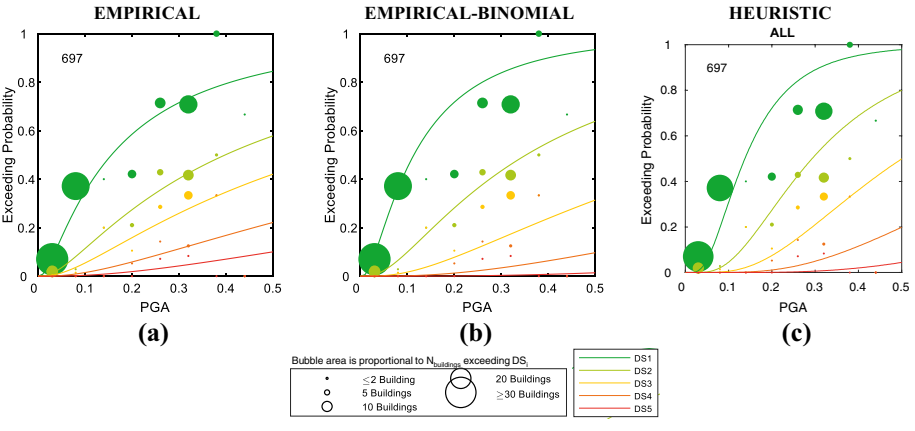

Fig. 18 Fragility curves for URM school buildings derived on the whole stock via the empirical (**a**), empirical-binomial (**b**) and heuristic (**c**) approaches, respectively

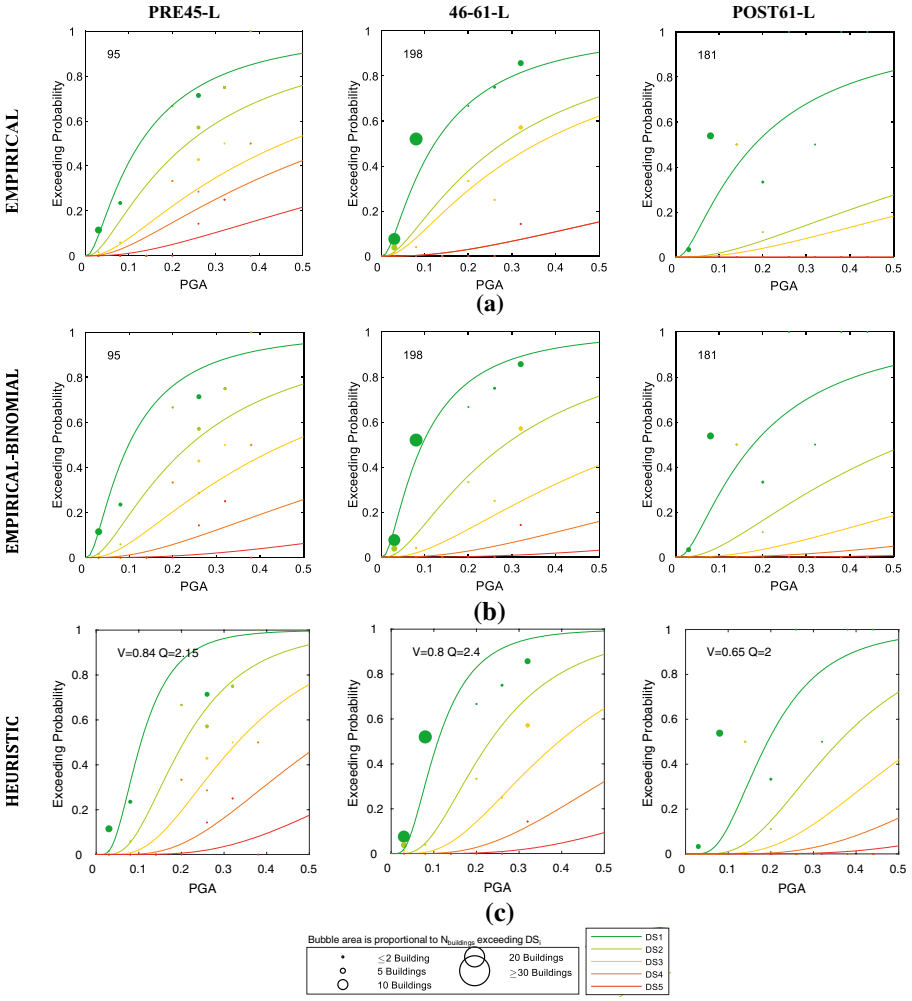

Fig. 19 Fragility curves for URM school buildings (groupings PRE45-L, 46-61-L, POST61-L): empirical (**a**), empirical-binomial (**b**) and heuristic approach (**c**)

Figure 18 shows that, overall, the fragility curves are able to capture well the trend of the real data, when the whole sample of buildings is considered.

Passing from Fig. 18 to Figs. 19 and 20, it is evident how splitting the observed data in classes by construction age and building height leads to irregular empirical probabilities of the different DSs, sometimes characterized by very few samples; in particular, this is evident for medium-rise buildings. This results in a greater difficulty in fitting the data, particularly when the pure empirical approach is adopted. Indeed, from Table 3 it emerges how, for this method, almost all parameters are missing in the medium-rise case. Moreover, for this case, differences higher than those found for RC school buildings arise also among the other two approaches.

In fact, the empirical-binomial approach solves the intrinsic inability of the empirical one associated with the almost complete absence of data, but it is anyway anchored to the

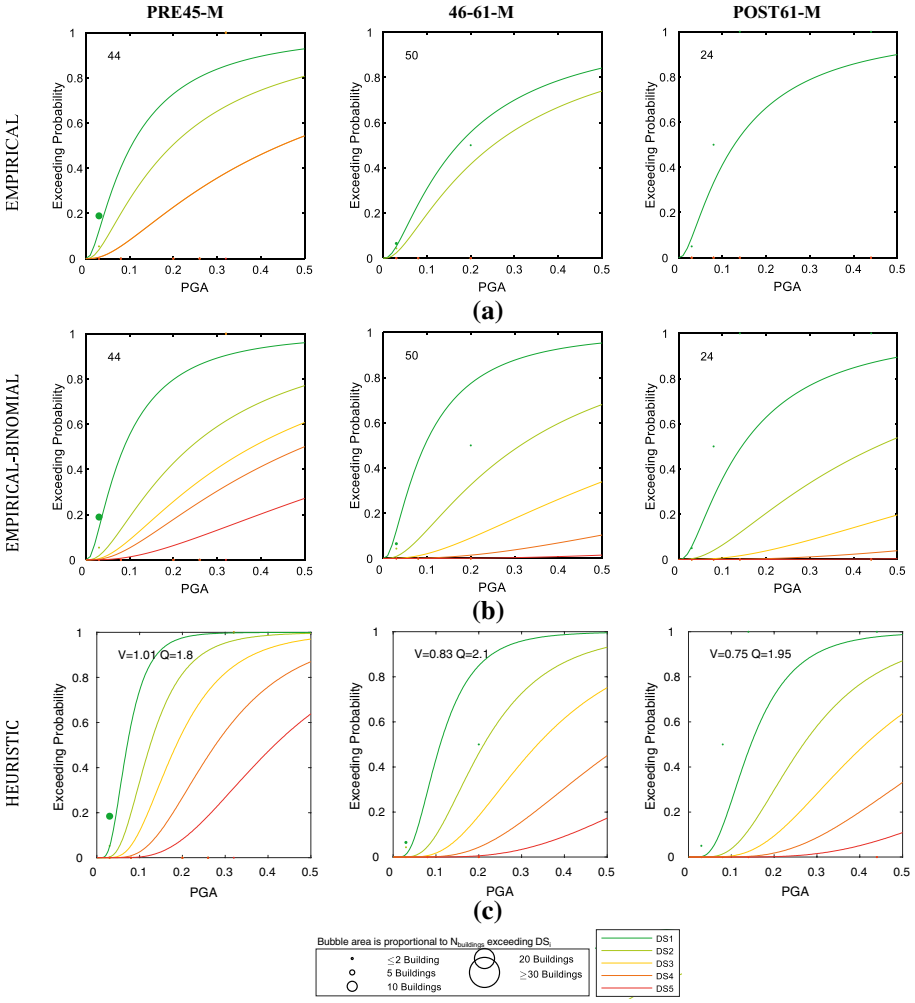

Fig. 20 Fragility curves for URM school buildings (groupings PRE45-M, 46-61-M, POST61-M): empirical (**a**), empirical-binomial (**b**) and heuristic approach (**c**)

observed damage even in the bins where very few data are available. As a matter of fact, the empirical-binomial approach works well when at least the estimate of the mean damage on each single PGA-bin may be considered reliable; for the URM medium-rise case, the mean value is sometime based on very few data (see the last PGA-bins in Fig. 11b).

Conversely, the heuristic one compensates the lack of samples by directly fitting the parameters (V and Q) that define the vulnerability curve, thus considering all together the data and assuming an heuristic increasing trend of the mean damage with the intensity; this allows to manage scattered irregularities in the trend of μ_D (e.g. as depicted in Fig. 13b in the case of the point referred to the last bin).

Regarding the values of the dispersion β, the comments reported in Sect. 4.2 are still valid. Moreover, it is worth noting that β values associated with the empirical and empirical-binomial approaches are slightly higher than those of RC school buildings confirming

Table 3 URM school buildings: median PGA (PGADSk, with $k = 1…5$), and dispersion β

Approach	Group	PGA_{DS1}	PGA_{DS2}	PGA_{DS3}	PGA_{DS4}	PGA_{DS5}	β
Empirical	ALL	0.16	0.40	0.63	1.21	2.17	1.15
	PRE45-L	0.13	0.23	0.46	0.61	1.16	1.07
	46-61-L	0.12	0.28	0.36	1.50	1.50	1.07
	POST61-L	0.18	0.95	1.32	–	–	1.07
	PRE45-M	0.10	0.20	0.45	0.45	–	1.07
	46-61-M	0.17	0.25	–	–	–	1.07
	POST61-M	0.13	–	–	–	–	1.07
Empirical-binomial	ALL	0.11	0.35	0.80	1.79	4.32	0.98
	PRE45-L	0.10	0.25	0.47	1.00	2.45	1.02
	46-61-L	0.10	0.30	0.66	1.43	3.47	1.02
	POST61-L	0.18	0.56	1.30	2.83	6.45	1.02
	PRE45-M	0.09	0.25	0.40	0.53	0.97	1.02
	46-61-M	0.12	0.50	1.59	4.64	15.48	1.02
	POST61-M	0.15	0.48	1.24	3.13	8.31	1.02
Heuristic	ALL	0.14	0.29	0.51	0.86	1.48	0.64
	PRE45-L	0.11	0.21	0.33	0.53	0.87	0.59
	46-61-L	0.11	0.23	0.39	0.67	1.15	0.61
	POST61-L	0.19	0.36	0.56	0.87	1.37	0.60
	PRE45-M	0.07	0.12	0.19	0.28	0.42	0.52
	46-61-M	0.11	0.21	0.34	0.54	0.86	0.63
	POST61-M	0.15	0.27	0.41	0.64	0.99	0.55

the higher scatter of URM sample. This is also ascribable to a bigger variability of URM structural features within the same class, as well as to a less robust statistics given the lower number of URM buildings, split across more sub-types, than those of RC buildings.

Finally, Fig. 21 illustrates the variation of seismic fragility across the adopted groupings (PRE45-L, 46-61-L, POST61-L, PRE45-M, 46–61-M, POST61-M), with reference only to the first three damage states. Focusing the attention on the empirical-binomial and heuristic approaches, due to the limitation of the pure empirical approach when applied to the URM sample, two observations emerge. For the low-rise buildings, both approaches highlight a decrease in the fragility from the oldest to the modern age (confirmed by all DSs). The decrease is more evident passing from 46–61 to POST61 rather than passing from PRE45 to 46–61. Such a result may be ascribed to the expected increase in the use of modern units (i.e. with the evolution of the concept of regular masonry) passing from 46–61 to POST61 (see also Fig. 6a), together with a small increase also in the percentage of HQD (non negligible even in the 45–61 age). Also, in the case of medium-rise buildings, for the heuristic approach, this trend is confirmed even if the distance among the ages is in some case a bit different. As a second observation, varying the height class (i.e. by comparing the dotted and the continuous lines), the heuristic approach estimates an increase of the vulnerability passing from the low-rise to medium-rise buildings, but this performance is not confirmed by the empirical-binomial approach for the age "45–61".

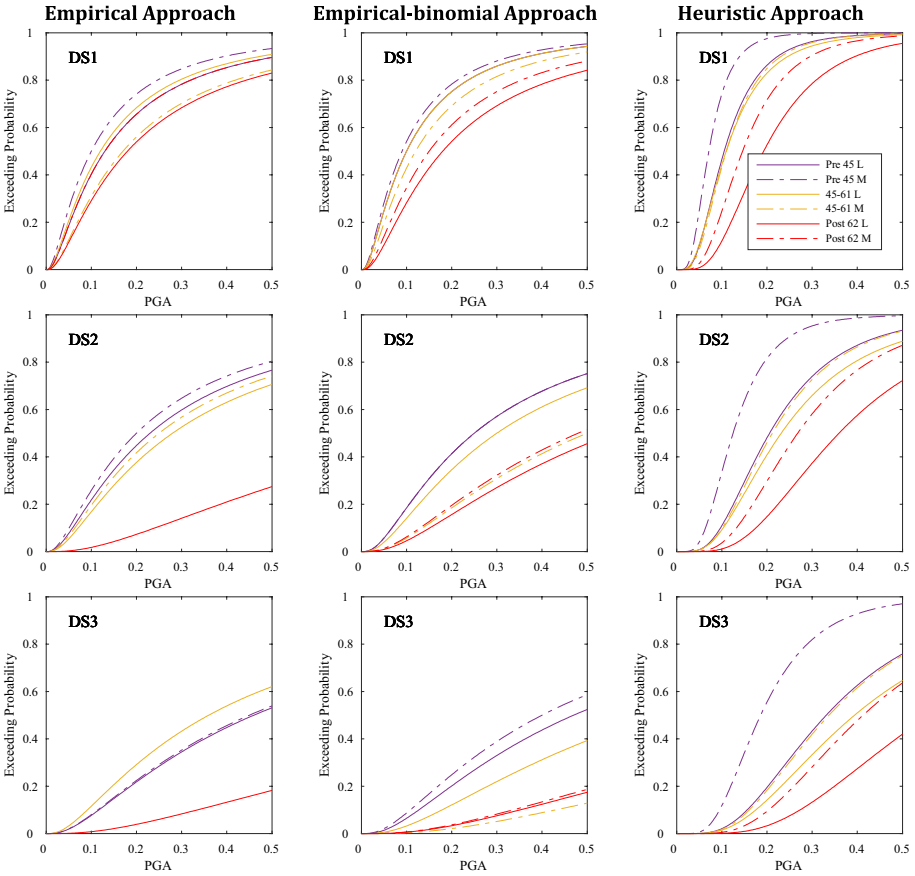

Fig. 21 Comparison of the seismic vulnerability of adopted groupings (PRE45-L, PRE45-M, 46–61-L, 46–61-M, POST61-L, POST61-M) captured by three adopted approaches

5 Comparison with available fragility curves of residential buildings

The available fragility curves for school buildings are very limited. In the literature, they have been mainly developed by using numerical or analytical-mechanical methods and often refer to other intensity measures (e.g. the spectral acceleration). The few works based on empirical approaches refer to buildings with structural features very different from those common in Italy (e.g. Nepal school buildings, in Giordano et al. 2021a, b).

Therefore, in this section a comparison is presented with fragility curves available in the literature for Italian residential buildings, which have been recently developed within the framework of the National Risk Assessment (NRA 2018) (Dolce and Prota 2021; Dolce et al. 2021). Such study involved the use of different models relying on various approaches to develop the fragility curves, namely: the pure empirical approach, referring to the data collected in the Da.D.O. platform (Rosti et al. 2021a for RC buildings, Rosti et al. 2021b and Zuccaro et al. 2021 for URM buildings); the analytical approach (Donà et al. 2021 for URM and Borzi et al. 2021 for RC buildings); the heuristic approach (Lagomarsino et al. 2021 for URM buildings). Even if the majority of fragility curves have been derived/

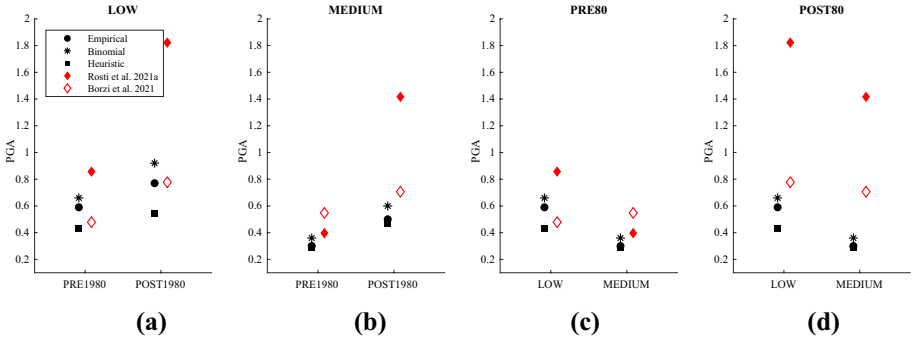

Fig. 22 Comparison of the median PGA_{DS3} (in g) values characterizing the fragility curves developed for the residential (in the context of NRA 2018) and school RC buildings (red markers refer to the residential buildings, while the black ones to the school buildings)

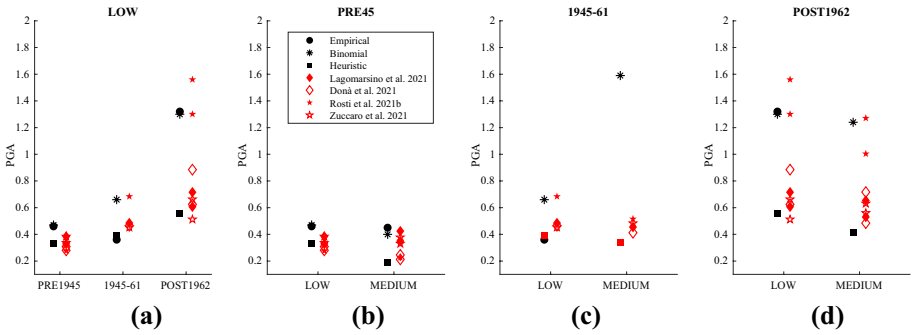

Fig. 23 Comparison of the median PGA_{DS3} (in g) values characterizing the fragility curves developed for the residential (in the context of NRA 2018) and school URM buildings (red markers refer to the residential buildings, while the black ones to the school buildings)

validated by the observed damage after L'Aquila earthquake (2009) as the school building stock here examined, it is worth noting that some differences can be found in the development process, i.e.: (1) the shake map proposed in Michelini et al. (2008) has been adopted for residential buildings while the updated one is used herein for school buildings (Michelini et al. 2020); (2) slightly different damage metrics have been used to convert the data collected in the AeDES form into the corresponding EMS-98 grades for residential buildings (i.e. Rota et al. 2008; Del Gaudio 2017 for RC residential buildings and Dolce et al. 2019 or Rota et al. 2008 for masonry ones in the field of empirical approaches).

A comparison is presented in Figs. 22 and 23, for the RC and URM building stocks respectively, with the aim of comparing the median PGA values associated with the fragility curves of DS3. In the Figures, the red markers refer to the residential buildings, the black ones to the school buildings while the shape distinguishes the method. Although, as discussed in previous sections, the comparison in terms of the PGA_{DS3} alone provides only a partial information on the overall set of fragility curves, the figures are useful to show a similar trend with age and height-rise.

Figures 24 and 25 show the comparison between the fragility curves for low-rise buildings, adopted in the NRA 2018 and those developed for school buildings. The colored

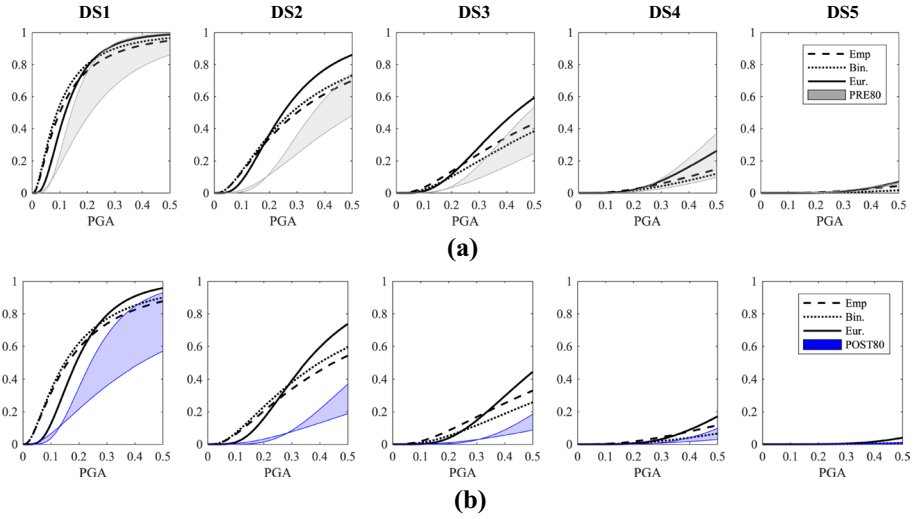

Fig. 24 Comparison between the fragility curves of low-rise RC buildings, developed for NRA 2018, and those of low-rise RC school buildings, varying the groupings PRE80 (**a**) and POST80 (**b**) and the damage states

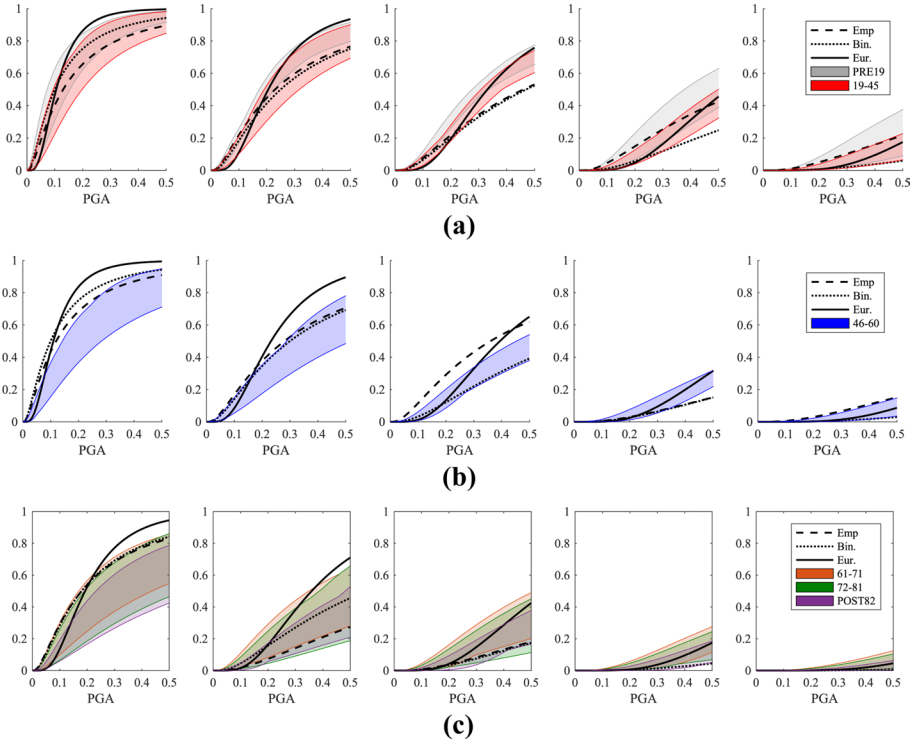

Fig. 25 Comparison between the fragility curves of low-rise URM buildings, developed for NRA 2018, and those of URM school buildings, varying the groupings PRE45 (**a**), 46-61 (**b**) and POST61 (**c**)

regions refer to the range of curves obtained by using the various methods adopted for residential buildings. Observations on medium-rise buildings would be similar, despite a less regular trend, as already observed due to the lower number of buildings in these datasets (figures are not included for the sake of conciseness). Figure 24 shows that for both RC groupings, PRE80 and POST80, the fragility curves of residential and school buildings are very similar for DS4 and DS5; by contrast, school buildings appear more vulnerable than residential ones in the case of slight to moderate damage. This is probably due to some specific architectural features of school buildings (e.g. large span between columns and large windows in infills), which make non-structural elements prone to damage (as already mentioned, damage to non-structural elements affect the first three DSs).

The comparison for low-rise UMR buildings (Fig. 25) shows that: (1) in the PRE45 class (Fig. 25a), fragility curves of school buildings match very well with those of residential buildings for the 19–45 age (this is coherent with the consistency of the school stock—see Fig. 5a); (2) in 46–61 (Fig. 25b) and POST61 (Fig. 25c) classes, a comparable vulnerability can be noticed for severe damage (the last three DSs), while for DS1 and DS2 school buildings appear to be a bit more vulnerable than the residential ones. Once again, as for RC buildings, this result may be due to distinctive architectural features of school building stock (e.g. higher inter-story height, greater distance between transversal walls, etc.).

In conclusion, both for RC and URM, school buildings turn out to be more vulnerable than residential ones for the first three DSs: at a first glance, this outcome is unexpected, because the hope is that schools are better quality buildings. However, it is worth noting that the post-earthquake damage assessment is made in a more accurate and precautionary way in the case of school buildings, due their social relevance.

6 Conclusions

This paper proposes fragility functions for reinforced concrete and masonry school buildings typical of the Italian construction standards, based on the post-earthquake data collected in the aftermath of the 2009 L'Aquila earthquake.

Significant effort was dedicated to collecting a complete database including all the school buildings (either damaged and undamaged) available in the Abruzzo region. To this end, data on buildings belonging to four different databases were analysed and merged in a unique dataset of 2037 records (1340 RC and 697 URM buildings).

Three different approaches (i.e. empirical, empirical-binomial, heuristic) have been used to derive the fragility curves, considering the entire dataset or specific building groupings. The results of the different approaches are discussed and compared. Finally, a direct comparison with other fragility curves available in the literature for the Italian residential buildings stock is carried out.

The main outcomes of this study may be summarized as follows:

- A critical review of the methods is performed, addressing the rationale behind the potential differences in the resulting parameters.
- The fragility curves derived for both RC and URM schools confirm the general hierarchy with the construction age and the number of storeys, namely increasing fragility with increasing height of the buildings and going back through the years.

- The comparison among fragility curves obtained by means of the different approaches is also used to test the robustness of the observational sample of data and the reliability of the hypothesis assumed in each of them.
- An overall coherence among fragility curves obtained by the three methods has been observed. It is not possible to state a priori which method is the best one, but this study highlighted the pros and cons of each of them. On the one hand, the pure empirical approach should be considered the reference one, but it is strongly influenced by the statistical representativity, as well as by the completeness and quality of the damage survey. On the other hand, the heuristic approach overcomes the lack of data but it may be somehow arbitrary in taking on a priori the progression between intensity and damage (ruled only by two free parameters, the vulnerability V and ductility Q indexes), as well as the binomial damage distribution for each value of the intensity (resulting in a regular predefined mutual distance between fragility curves of the different damage states). This latter feature is also at the base of the empirical-binomial approach.
- The comparison with the fragility functions of the Italian residential buildings, available in the literature, highlights a very similar performance of the two building stocks, with a slightly higher vulnerability of school buildings with reference to the first damage states.

Finally, the result of this study refers to school buildings of the Abruzzo region that may not fully represent the peculiarities of the entire population of the Italian schools, despite the good agreement in terms of the general building characteristics. Other uncertainties may arise from the correlation of the damage with the seismic intensity, since the available data only refer to the damage observed in the aftermath of the 2009 L'Aquila earthquake.

Acknowledgements The study presented in the paper was developed within the research activities carried out in the frame of 2019–2021 ReLUIS Project—WP4 Seismic Risk Maps (MARS) (Coordinators: Sergio Lagomarsino and Angelo Masi). The project has been funded by the Italian Department of Civil Protection. Note that the opinions and conclusions presented by the authors do not necessarily reflect those of the funding entity.

Authors' contributions MDL/SC/SL/GMV/AP: conceptualization, methodology; CDV/CDG/DO: formal analysis and investigation; SC/CDV/CDG: writing–original draft, preparation; MDL/SL/GMV: writing-review and editing; MDL/SC/SL/GMV/AP: resources, supervision.

Funding Open access funding provided by Università degli Studi di Genova within the CRUI-CARE Agreement. The research activity presented in this paper, did not receive any grant from funding agencies in the public, commercial or not-for-profit sectors that may gain or lose financially through publication of this work.

Declarations

Conflict of interest The authors declare that they have no known competing financial interests or personal relationships that could have appeared to influence the work reported in this paper.

References

Applied Technology Council Report ATC-13 (1985) Earthquake damage evaluation data for California. Palo Alto

Applied Technology Council Report ATC-40 (1996) Seismic evaluation and retrofit of concrete buildings. Redwood City

Architectural Institute of Japan (1995) Preliminary report of the 1995 Hyogoken-Nanbu Earthquake, (English edition). Tokyo

Augenti N, Cosenza E, Dolce M, Manfredi G, Masi A, Samela L (2004) Performance of school buildings during the 2002 Molise, Italy. Earthq Earthq Spectra 20(1):257–270. https://doi.org/10.1193/1.1769374

Azizi-Bondarabadi H, Mendes N, Lourenço PB (2016) Sadeghi NH (2016) Empirical seismic vulnerability analysis for masonry buildings based on school buildings survey in Iran. Bull Earthqe Eng 14:3195–3229. https://doi.org/10.1007/s10518-016-9944-1

Baggio C, Bernardini A, Colozza R, Corazza L, Della Bella M, Di Pasquale G, Goretti A, Martinelli A, Orsini G, Papa F, Zuccaro G (2007) Field manual for post-earthquake damage and safety assessment and short term countermeasures (AeDES). European Commission—Joint Research Centre—Institute for the Protection and Security of the Citizen, EUR, 22868

Baker JW, Cornell CA (2005) A vector-valued ground motion intensity measure consisting of spectral acceleration and epsilon. Earthq Eng Struct Dyn 34:1193–1217. https://doi.org/10.1002/eqe.474

Baraschino R, Baltzopoulos G, Iervolino I (2020) (2020) R2R-EU: Software for fragility fitting and evaluation of estimation uncertainty in seismic risk analysis. Soil Dyn Earthq Eng 132:106093. https://doi.org/10.1016/j.soildyn.2020.106093

Borzi B, Faravelli M, Di Meo A (2021) Application of the SP-BELA methodology to RC residential buildings in Italy to produce seismic risk maps for the national risk assessment. Bull Earthq Eng 19(8):3185–3208. https://doi.org/10.1007/s10518-020-00953-6

Braga F, Dolce M, Liberatore D (1982) A statistical study on damaged buildings and an ensuing review of the MSK-76 scale. In: Proceedings of the 7th European conference on earthquake engineering, Athens, Greece, pp 431–450

Cattari S, Angiolilli M (2022) Multiscale procedure to assign structural damage levels in masonry buildings from observed or numerically simulated seismic performance. Bull Earthq Eng 20(13):7561–7607. https://doi.org/10.1007/s10518-022-01504-x

Cattari S, Alfano S, Masi A, Manfredi V, Borzi B, Di Meo A, Da Porto F, Saler E, Dall'Asta A, Gioiella L, Di Ludovico M, Del Vecchio C, Gattesco N, Verderame G, Del Gaudio C (2022) Risk assessment of Italian School buildings at national scale: the MARS project experience, Proceedings of 3rd European Conference on Earthquake Engineering and Seismology, 3ECEES, Bucharest, Romania, September 4th to 9th 2022

Charvet I, Ioannou I, Rossetto T, Suppasri A, Imamura F (2014) Empirical fragility assessment of buildings affected by the 2011 Great East Japan tsunami using improved statistical models. Nat Hazards 73(2):951–973

Chiarabba C, Amato A, Anselmi M, Baccheschi P, Bianchi I, Cattaneo M et al (2009) The 2009 L'Aquila (central Italy) MW6.3 earthquake: Main shock and aftershocks. Geophys Res Lett. https://doi.org/10.1029/2009GL039627

D'Ayala D, Galasso C, Nassirpour A, Adhikari RK, Yamin L, Fernandez R, Lo D, Garciano L, Oreta A (2020) Resilient communities through safer schools. Int J Disaster Risk Reduct. https://doi.org/10.1016/j.ijdrr.2019.101446

Decision No 1313 (2013) EU of the European Parliament and of the Council of 17 December 2013 on a Union Civil Protection Mechanism. Official Journal of the European Union, L.347/294

De Martino G, Di Ludovico M, Prota A, Moroni C, Manfredi G, Dolce M (2017) Estimation of repair costs for RC and masonry residential buildings based on damage data collected by post-earthquake visual inspection. Bull Earthq Eng 15(4):1681–1706. https://doi.org/10.1007/s10518-016-0039-9

Del Gaudio C, De Martino G, Di Ludovico M, Manfredi G, Prota A, Ricci P, Verderame GM (2017) Empirical fragility curves from damage data on RC buildings after the 2009 L'Aquila earthquake. B Earthq Eng 15:1425–1450. https://doi.org/10.1007/s10518-016-0026-1

Del Gaudio C, Di Ludovico M, Polese M, Manfredi G, Prota A, Ricci P, Verderame GM (2020) Seismic fragility for Italian RC buildings based on damage data of the last 50 years. Bull Earthq Eng 18(5):2023–2059. https://doi.org/10.1007/s10518-020-00890-4

Del Gaudio C, Scala SA, Ricci P (2021) Verderame MG (2021) Evolution of the seismic vulnerability of masonry buildings based on the damage data from L'Aquila 2009 event. Bullet Earthq Eng 19:4435–4470. https://doi.org/10.1007/s10518-021-01132-x

Del Vecchio C, Ludovico MD, Prota A (2020) Repair costs of reinforced concrete building components: from actual data analysis to calibrated consequence functions. Earthq Spectra 36(1):353–377. https://doi.org/10.1177/8755293019878194

Di Ludovico M, Prota A, Moroni C, Manfredi G, Dolce M (2017) Reconstruction process of damaged residential buildings outside historical centres after the L'Aquila earthquake: part II—"heavy damage" reconstruction. Bull Earthq Eng15(2):693–729

Di Ludovico M, Digrisolo A, Moroni C, Graziotti F, Manfredi V, Prota A, Dolce M, Manfredi G (2019a) Remarks on damage and response of school buildings after the Central Italy earthquake sequence. Bull Earthq Eng 17:5679–5700. https://doi.org/10.1007/s10518-018-0332-x

Di Ludovico M, Santoro A, De Martino G, Moroni C, Prota A, Dolce M, Manfredi G (2019b) Cumulative damage to school buildings following the 2016 central Italy earthquake sequence. Bollettino Di Geofisica Teorica Ed Applicata 60(2):165–182. https://doi.org/10.4430/bgta0240

Dolce M, Goretti A (2015) Building damage assessment after the 2009 Abruzzi earthquake. Bull Earthq Eng 13(8):2241–2264. https://doi.org/10.1007/s10518-015-9723-4

Dolce M, Prota A (2021) Guest editorial to the special issue—seismic risk assessment in Italy. Bull Earthq Eng 19(8):2995–2998. https://doi.org/10.1007/s10518-021-01107-0

Dolce M, Speranza E, Giordano F, Borzi B, Bocchi F, Conte C, Di Meo A, Faravelli M, Pascale V (2019) Observed damage database of past Italian earthquakes the Da.D.O. Webgis Bollettino Di Geofisica Teorica e Applicata 60(2):141–164. https://doi.org/10.4430/bgta0254

Dolce M, Prota A, Borzi B, da Porto F, Lagomarsino S, Magenes G et al (2021) Seismic risk assessment of residential buildings in Italy. Bull Earthq Eng 19(8):2999–3032. https://doi.org/10.1007/s10518-020-01009-5

Donà M, Carpanese P, Follador V, Sbrogiò L, da Porto F (2021) Mechanics-based fragility curves for Italian residential URM buildings. Bull Earthq Eng 19(8):3099–3127. https://doi.org/10.1007/s10518-020-00928-7

Federal Emergency Management Agency (1997) NEHRP Guidelines for seismic rehabilitation of buildings. Federal Emergency Management Agency Report: FEMA 273. Washington D.C

Federal Emergency Management Agency (1999) HAZUS user and technical manuals. Federal Emergency Management Agency Report: HAZUS 1999, Washington, D.C., Vol. 7

Federal Emergency Management Agency (FEMA) (2012) Hazus-MH 2.1 technical manual: earthquake model

Gautam G, Adhikari R, Rupakhety R, Koirala P (2020) An empirical method for seismic vulnerability assessment of Nepali school buildings. Bull Earthq Eng 18:5965–5982. https://doi.org/10.1007/s10518-020-00922-z

Giordano N, De Luca F, Sextos A et al (2021a) Empirical seismic fragility models for Nepalese school buildings. Nat Hazards 105:339–362. https://doi.org/10.1007/s11069-020-04312-1

Giordano N, De Luca F, Sextos A (2021b) Analytical fragility curves for masonry school building portfolios in Nepal. Bull Earthq Eng 19:1121–1150. https://doi.org/10.1007/s10518-020-00989-8

Giovinazzi S, Lagomarsino S (2005). Fuzzy-random approach for a seismic vulnerability model. In: Proceedings of the ICOSSAR2005 safety and reliability of engineering systems and structures. Rome, Italy, Millpress, Rotterdam, ISBN 90-5966-040 0, pp 2879–2887

González C, Niño M, Jaimes MA (2020) Event-based assessment of seismic resilience in Mexican school buildings. Bull Earthq Eng 18:6313–6336. https://doi.org/10.1007/s10518-020-00938-5

Goretti A, Di Pasquale G (2004) Building inspection and damage data for the 2002 Molise, Italy, earthquake. Earthq Spectra 20(S1):S167–S190. https://doi.org/10.1193/1.1769373

Grant DN, Bommer JJ, Pinho R, Calvi GM, Goretti A, Meroni F (2007) A prioritization scheme for seismic intervention in school buildings in Italy. Earthq Spectra 23:291–314. https://doi.org/10.1193/1.2722784

Grünthal G, Musson RMW, Schwarz J, Stucchi M (1998) European Macroseismic Scale. Cahiers du Centre Européen de Géodynamique et de Séismologie, Vol. 15-European Macroseismic Scale 1998. European Center for Geodynamics and Seismology, Luxembourg. ISBN No 2-87977-008-4

Grünthal G, Musson R, Schwarz J, Stucchi M (1998) European macroseismic scale 1998. In: Cahiers de Centre Européen de Géodynamique et de Seismologie, vol 15. Luxembourg

Hannewald P, Michel C, Lestuzzi P, Crowley C, Pinguet J, Fäh D (2020) Development and validation of simplified mechanics-based capacity curves for scenario-based risk assessment of school buildings in Basel. Eng Struct. https://doi.org/10.1016/j.engstruct.2020.110290

National Risk Assessment (NRA 2018) Overview of the potential major disasters in Italy. Issued by the Italian Civil Protection Department. Updated December 2018

Kita A, Cavalagli N, Masciotta MG, Lourenço PB, Ubertini F (2020) Rapid post-earthquake damage localization and quantification in masonry structures through multidimensional non-linear seismic IDA. Eng Struct 219:110841

Lagomarsino S, Giovinazzi S (2006) Macroseismic and mechanical models for the vulnerability and damage assessment of current buildings. Bull Earthq Eng 4(4):415–443. https://doi.org/10.1007/s10518-006-9024-z

Lagomarsino S, Cattari S, Ottonelli D (2021) The heuristic vulnerability model: fragility curves for masonry buildings. Bull Earthq Eng 19(8):3129–3163. https://doi.org/10.1007/s10518-021-01063-7

Lallemant D, Kiremidjian A, Burton H (2015) Statistical procedures for developing earthquake damage fragility curves. Earthq Eng Struct Dyn 44:1373–1389

Luco N, Cornell CA (2007) Structure-specific scalar intensity measures for near-source and ordinary earthquake ground motions. Earthq Spectra 23(2):357–392. https://doi.org/10.1193/1.2723158

Martins L, Silva V (2021) Development of a fragility and vulnerability model for global seismic risk analyses. Bull Earthq Eng 19(15):6719–6745. https://doi.org/10.1007/s10518-020-00885-1

Masi A, Lagomarsino S, Dolce M, Manfredi V, Ottonelli D (2021) Towards the updated Italian seismic risk assessment: exposure and vulnerability modelling. Bull Earthq Eng 19(8):3253–3286. https://doi.org/10.1007/s10518-021-01065-5

Michelini A, Faenza L, Lauciani V, Malagnini L (2008) ShakeMap implementation in Italy. Seismol Res Lett 79(5):688–697

Michel C, Hannewald P, Lestuzzi P, Fäh D, Husen S (2017) Probabilistic mechanics-based loss scenarios for school buildings in Basel (Switzerland). Bull Earthq Eng 15:1471–1496. https://doi.org/10.1007/s10518-016-0025-2

Michelini A, Faenza L, Lanzano G, Lauciani V, Jozinović D, Puglia R, Luzi L (2020) The new ShakeMap in Italy: progress and advances in the last 10 yr. Seismol Res Lett 91(1):317–333. https://doi.org/10.1785/0220190130

Minas S, Galasso C (2019) Accounting for spectral shape in simplified fragility analysis of case-study reinforced concrete frames. Soil Dyn Earthq Eng 119:91–103

MIUR Italian Ministry of Instruction, University and Research (2004) Database of school buildings

Muñoz A, Blondet M, Aguilar R, Astorga MA (2007) Empirical fragility curves for Peruvian school buildings. ERES. https://doi.org/10.2495/ERES070261

Nakano Y (2020) Damage assessment activities of school buildings after recent major earthquakes in Japan. In: Proceedings of the 17 WCEE, Sendai, Japan, paper n. C002595

OECD Programme on Educational Building (PEB) (2004) Keeping schools safe in earthquakes. https://doi.org/10.1787/9789264063549-zh

Rossetto T, D'Ayala D, Ioannou I, Meslem A, Pitilakis K, Crowley H, Kaynia AM (2014) SYNER-G: typology definition and fragility functions for physical elements at seismic risk. In: Geotechnical, geological and earthquake engineering, vol. 27, Springer, Netherlands. https://doi.org/10.1007/978-94-007-7872-6

Rota M, Penna A, Strobbia CL (2008) Processing Italian damage data to derive typological fragility curves. Soil Dyn Earthq Eng 28:933–947. https://doi.org/10.1016/j.soildyn.2007.10.010

Rosti A, Rota M, Penna A (2018) Damage classification and derivation of damage probability matrices fromL'Aquila (2009) post-earthquake survey data. Bull Earthq Eng 16(9):3687–3720

Rosti A, Del Gaudio C, Di Ludovico M, Magenes G, Penna A, Polese M et al (2020) Empirical vulnerability curves for Italian residential buildings. Bollettino Di Geofisica Teorica Ed Applicata 61(3):357–374. https://doi.org/10.4430/bgta0311

Rosti A, Del Gaudio C, Rota M, Ricci P, Di Ludovico M, Penna A, Verderame GM (2021a) Empirical fragility curves for Italian residential RC buildings. Bull Earthq Eng 19(8):3165–3181. https://doi.org/10.1007/s10518-020-00971-4

Rosti A, Rota M, Penna A (2021b) Empirical fragility curves for Italian URM buildings. Bull Earthq Eng 19:3057–3076. https://doi.org/10.1007/s10518-020-00845-9

Sabetta F, Goretti A, Lucantoni A (1998) Empirical fragility curves from damage surveys and estimated strong ground motion. In: Proceedings of the 11th European conference earthquake engineering, Balkema, Rotterdam

Sieberg A (1930) Geologie der Erdbeben. Handbuch Der Geophysik 2(4):552–555

Silva V, Akkar S, Baker J et al (2019) Current challenges and future trends in analytical fragility and vulnerability modeling. Earthq Spectra 35(4):1927–1952. https://doi.org/10.1193/042418EQS101O

Silva V, Amo-Oduro D, Calderon A et al (2020) Development of a global seismic risk model. Earthq Spectra 36(1_suppl):372–394. https://doi.org/10.1177/8755293019899953

Spence R, Martínez-Cuevas S, Baker H (2021) Fragility estimation for global building classes using analysis of the Cambridge earthquake damage database (CEQID). Bull Earthq Eng 19:5897–5916. https://doi.org/10.1007/s10518-021-01178-x

Taylor G, Ventura CE, Pina FE, Finn WDL (2010) Performance-based retrofit of school buildings in British Columbia, Canada. In: ATC and SEI conference on improving the seismic performance of existing buildings and other structures December 9–11, 2009 | San Francisco, California, United States

UNISDR (2014) Comprehensive School Safety, United Nations Office for Disaster Risk Reduction (UNDRR)

Wang Y, Goettel KA (2007) Enhanced rapid visual screening (E-Rvs) method for prioritization of seismic retrofits in Oregon. Oregon Department of Geology and Mineral Industries Special Paper 39 Published in conformance with ORS 516.030

WISS (2013) Worldwide initiative for safe schools—vision: by 2030, Every School Will Be Safe, United Nations Office for Disaster Risk Reduction (UNDRR)

Yekrangnia M, Bakhshi A, Ghannad MA, Panahi M (2021) Risk assessment of confined unreinforced masonry buildings based on FEMA P-58 methodology: a case study—school buildings in Tehran. Bull Earthq Eng 19:1079–1120. https://doi.org/10.1007/s10518-020-00990-1

Zuccaro G, Perelli FL, De Gregorio D, Cacace F (2021) Empirical vulnerability curves for Italian mansory buildings: evolution of vulnerability model from the DPM to curves as a function of acceleration. Bull Earthaq Eng 19(8):3077–3097. https://doi.org/10.1007/s10518-020-00954-5

Zucconi M, Sorrentino L, Ferlito R (2017) Principal component analysis for a seismic usability model of unreinforced masonry buildings. Soil Dyn Earthq Eng 96:64–75. https://doi.org/10.1016/j.soildyn.2017.02.014

Authors and Affiliations

Marco Di Ludovico[1] · Serena Cattari[2] · Gerardo Verderame[1] · Ciro Del Vecchio[3] · Daria Ottonelli[2] · Carlo Del Gaudio[1] · Andrea Prota[1] · Sergio Lagomarsino[2]

Marco Di Ludovico
diludovi@unina.it

Gerardo Verderame
verderam@unina.it

Ciro Del Vecchio
cdelvecchio@unisannio.it

Daria Ottonelli
daria.ottonelli@unige.it

Carlo Del Gaudio
carlo.delgaudio@unina.it

Andrea Prota
aprota@unina.it

Sergio Lagomarsino
sergio.lagomarsino@unige.it

[1] Department of Structures for Engineering and Architecture, University of Naples Federico II, Via Claudio 21, 80125 Naples, Italy

[2] Department of Civil, Chemical and Environmental Engineering (DICCA), University of Genoa, Via Montallegro 1, 16145 Genoa, Italy

[3] Department of Engineering (DING), University of Sannio, Piazza Roma 21, 82100 Benevento, Italy